

21 JUN 1988

MAY, 1988

VOLUME 19

NUMBER 1

NEWSLETTER

INDEX

	<u>page</u>
From the Editor's desk	1
<u>Contributions</u>	
BASF	3
D. C. Blackley	4
F. Candau	6
M. D. Croucher	69
A. S. Dunn	7
M. S. El-Aasser	9
V. I. Eliseeva	16, 21
A. P. Gast	24
A. E. Hamielec	26, 41
S. C. JOHNSON	29
J. Lyklema	35
D. H. Napper	38
R. Pelton	41
C. Pichot	42
I. Piirma	43
G. W. Poehlein	45
POLYSAR	56
ROHM & HAAS	58
R. L. Rowell	59
W. B. Russel	60
V. T. Stannett	62
D. C. Sundberg	63
J. W. Vanderhoff	9
A. Vrij	65
J. Ugelstad	67
M. A. Winnik	69

FROM THE EDITOR'S DESK

Contributions

Professor Eliseeva's contribution for the last Newsletter arrived after the Newsletter was dispatched. It was held over until this time and appears with her current contribution. David Blackley's contribution for the September, 87 volume was lost *en route* and appears here in an updated version.

Conferences

The NATO Advanced Study Institute on Polymer Colloids will be held 3-15 July in Strasbourg. Lecturers will include Candau, Croucher, El-Aasser, Fitch, Goodwin, Ottewill, Pusey, Rowell, Tadros, Vanderhoff, van de Ven and Winnik. The areas covered will include emulsion and inverse emulsion and dispersion polymerization, modern techniques for the study of polymer colloids, as well as their applications, especially in the biosciences. Further details from Mrs. M. J. Proctor, School of Chemistry, University of Bristol, Cantock's Close, Bristol BS8 1TS, UK.

The 11th Annual Short Course on Advances in Emulsion Polymerization and Latex Technology is to be held in Davos, Switzerland, 22-26 August, 1988. The course presents an in-depth study of the synthesis, characterization and properties of latices. Further details from Dr. Gary Poehlein, Graduate Office (Savant), Georgia Institute of Technology, Atlanta, GA 30332-0265, USA.

The Colloid and Interface Science Group of the Faraday Division, Royal Society of Chemistry is to hold two meetings relevant to polymer colloids in 1988. First, a research style conference on Structure in Colloidal Systems and its Characterization at the University of Bath, 21-23 September. Short contributions followed by longer discussion periods are envisaged. Further details from Dr. Jim Goodwin, School of Chemistry, University of Bristol, Cantock's Close, Bristol BS8 1TS, U.K. Then a meeting on Aggregation in Colloidal Dispersions to be held in conjunction with the AGM at the Scientific Societies' Lecture Theatre, Saville Row, London on 16 December. This will concentrate on the process of aggregation of particulate dispersions with presentations on the effects of shear on aggregate structures, control of aggregate morphology and sedimentation behaviour in aggregated dispersions. Further information from Dr. R. Buscall, Corporate Colloid Science Group, ICI, The Heath, Runcorn, UK.

The Second International Symposium on Copolymerization and Copolymers in Dispersed Media will be held in Lyon, France, 3-7 April, 1989. Invited speakers include Barton, Blackley, Candau, Cavaille, Gilbert, Hamielec, Fitch, Daniel, Ottewill, Ross, Piirma, El-Aasser, Zozel, Nomura, Okubo, Brooks, Ober, Yeliseeva and Vanderhoff. Further details from the organizers: Professors J. Guillot/C. Pichot, Laboratoire des Matériaux Organiques, BP24-69390 Vernaison, France.

A call for papers has been made for the PRI organized conference entitled Polymer Latex III. This follows on the successful conferences in 1978 and 1985. It is to be held at the City Conference Centre, London EC3, on 27-28 June, 1989. John Vanderhoff will be the keynote speaker. Further details: Conference Centre, PRI, 11 Hobart Place, London SW1W 0HL, UK.

The 7th Gordon Conference on Polymer Colloids is to be organized by Irja Piirma. Please note the date: 10-15 July 1989. Also, don't forget the PAC-CHEM Conference in Honolulu in December, 1989.

Next Newsletter

Contributions for the next Newsletter to be forwarded to me by AIRMAIL by 31 August, 1988.

D. H. Napper
Editor

Dr. Hans Kast c/o

BASF Aktiengesellschaft · D-6700 Ludwigshafen

Contribution to Polymer Colloids Newsletter**ON PARTICLE COALESCENCE IN LATEX FILMS II**

(K. HAHN, G. LEY, R. OBERTHÜR)

The particle coalescence in latex films is investigated by measuring the "smearing out process" of perdeuterated nPBMA latex particles in a matrix of protonated nPBMA using SANS. It is found, that - at least in this system - there is massive interdiffusion of material of different latex particles. Diffusion constants for 70 °C and 90 °C tempering temperature are determined. In addition the effect of molecular mass, crosslinking and incompatibility of the matrix material is investigated. As expected the interdiffusion decreases with increasing molecular mass, but - surprisingly - dense crosslinking of the matrix latex particles accelerates the smearing out process. Increasing incompatibility lowers the rate of the smearing out process.

submitted to: Colloid & Polymer Science 1988

FURTHER INFORMATION CONCERNING NOVEL INITIATOR/STABILISERS
FOR AQUEOUS EMULSION POLYMERISATION REACTIONS

D. C. Blackley, London School of Polymer Technology,
The Polytechnic of North London, Holloway, London N7 8DB.

Following our contribution to a previous issue of the Polymer Colloid Group Newsletter concerning the preparation and properties of a novel series of azo initiator/stabilisers for the initiation of aqueous emulsion polymerisation reactions in the absence of other colloid stabilisers, we have received enquiries for further information about the preparation and characterisation of these initiator/stabilisers. Although we intend to submit a full account of this investigation for publication during the next few months, we thought that it might be useful to interested fellow-workers to have some further information concerning the preparation and characterisation of the initiator/stabilisers rather sooner by way of our contribution to the current issue of the Newsletter.

The starting materials for the preparation of the initiator/stabilisers were a range of fatty-alcohol ethoxylates based upon a mixture of cetyl and oleyl alcohols, and 4,4'-azobis-4-cyanopentanoic acid (4,4'-AB-4-CPA). The fatty-alcohol ethoxylates were commercial materials (the "Texafor A" series supplied by ABM Chemicals). They were used as received. The 4,4'-AB-4-CPA was either purchased as such or prepared by a procedure in which 1 mole of sodium cyanide and 0.5 mole of hydrazine sulphate were dissolved in 500 cm³ of water at 50°C, and to this solution was added over a period of 30 minutes a solution of 1 mole of laevulinic acid and 1 mole of sodium hydroxide in 200 cm³ of water. The solution was stirred vigorously, and bromine added until the solution was deep yellow in colour. The excess bromine was removed by adding sodium hydrogen sulphite until the colour was white/pale yellow. The white solid which had precipitated was collected and washed once with iced water. The yield was 42%. The dried solid melted over the range 118-128°C (literature range 115-127°C).

The diacid chloride of 4,4'-AB-4-CPA was prepared by reacting 0.1 mole of 4,4'-AB-4-CPA with 0.3 mole of phosphorus pentachloride in 300 cm³ of benzene. The mixture was allowed to stand in an ice bath for 30 minutes, and then for 2 hours at room temperature. The solution was filtered and dried using a rotary evaporator. The product was a pale-yellow solid. This solid was washed twice with a 1:3 mixture of diethyl ether and hexane. The solid was then dissolved in the minimum volume of dichlorohexane, and the diacid chloride precipitated by adding hexane. The product was a white solid of pungent odour. The yield was 65%. The product has been characterised by elemental analysis, infrared spectroscopy, ¹³C NMR spectroscopy, and mass spectroscopy. The characterisation data for the batches of compound used to prepare the derivatives of the fatty-alcohol ethoxylates are consistent with the compound having been the expected diacid chloride of 4,4'-AB-4-CPA. However, it should be noted that sometimes we obtained products which appeared to differ significantly from the expected diacid chloride, and which yielded derivatives with aliphatic alcohols which had unexpected properties. Neither we nor the organic chemists with whom we have discussed this problem have been able to offer any plausible reason for the formation of two types of product from this reaction. Nor do we know

what determines which product is obtained from any particular reaction, because, as far as we know, the reaction conditions were identical in all cases. We will be most interested to hear if any fellow-workers have similar experiences, particularly if they are able to suggest a plausible structure for the second product and offer a convincing explanation for the formation of the two different products on different occasions under virtually identical reaction conditions!

The initiator/stabilisers were then prepared by reacting 1 mole of the diacid chloride with 2 moles of fatty-alcohol ethoxylate and 2 moles of triethylamine in 300 cm³ of toluene at room temperature for one hour. A precipitate of triethylammonium chloride formed almost immediately. This precipitate was removed by filtration, and the desired derivatives isolated by evaporating the toluene at 35°C using a rotary evaporator. The derivatives were obtained as white waxes in near-theoretical yield. They were used without further purification. The infrared spectra of compounds obtained by reacting the diacid chloride of 4,4'-AB-4-CPA with hydroxy compounds are consistent with those compounds being the expected esters of 4,4'-AB-4-CPA.

The ultraviolet absorption spectra of the fatty-alcohol ethoxylate derivatives are consistent with them being the expected azo compounds. The kinetics of the thermal decomposition of these derivatives in water were determined by following the decrease in the intensity of the ultraviolet absorption at 350 nm. The initial concentration of azo groups was determined from the absorption after heating the solution at 70°C until the absorption underwent no further change. Satisfactory first-order plots for the decomposition were obtained for each of the derivatives at all the temperatures investigated. Typical results (for the derivative obtained from the 30-mole ethoxylate) are as follows:

<u>temperature/°C</u>	<u>k_d/s⁻¹</u>
50	3.24×10 ⁻⁶
60	1.02×10 ⁻⁵
65	1.80×10 ⁻⁵
70	3.09×10 ⁻⁵

In all cases, satisfactory Arrhenius plots for log k_d v. T⁻¹ were obtained, from which the following activation energies were calculated:

derivative from 24-mole ethoxylate : 164 kJ mol⁻¹
 derivative from 30-mole ethoxylate : 132 kJ mol⁻¹
 derivative from 45-mole ethoxylate : 105 kJ mol⁻¹
 derivative from 60-mole ethoxylate : 135 kJ mol⁻¹

Contribution from the Institut Charles Sadron (CRM-EAHP) CNRS-ULP
8, rue Boussingault, 67083 Strasbourg Cedex

by

F. CANDAU

EFFECTS OF SOLUTIONS COMPONENTS ON THE TERMINATION MECHANISM IN ACRYLAMIDE
MICROEMULSION POLYMERIZATIONS

(M. Carver, F. Candau, R.M. Fitch)

A study of the effect of the various solution components on the kinetics of the polymerization of acrylamide in toluene/AOT/H₂O microemulsions has been performed. For the polymerizations with toluene as the continuous phase, both the rate of polymerization, R_p , and the molecular weight of the polyacrylamide were found to be first order in monomer concentration. Furthermore, for the low temperatures (10°C) involved in these experiments, nondegradative chain transfer to monomer appears to be insignificant.

When the continuous phase solvent was changed, an exponential dependence, X , of R_p on the incident light intensity in the order of benzene ($X = 0.55$) < heptane ($X = 0.73$) < toluene ($X = 1.06$) was found. This order corresponds to the increasing susceptibility of the hydrogen atoms in the solvent molecules to abstraction by free radicals. Thus, the monoradical termination found in toluene microemulsions is due to the ease with which benzyl radicals can be formed, and the unlikelihood that they will reinitiate polymerization. In benzene, on which there are no labile hydrogen atoms, termination is a biradical process. Though termination by AOT cannot be directly ruled out, the evidence indicates that little, if any, degradative chain transfer to AOT is occurring.

RECENT PUBLICATIONS

C. Holtzscherer, J.P. Durand and F. Candau.

"Polymerization of acrylamide in nonionic microemulsions : characterization of the microlatices and polymers formed".
Colloid Polym. Sci., 265, 1067 (1987).

C. Holtzscherer and F. Candau.

"Application of the cohesive energy ratio concept (CER) to the formation of polymerizable microemulsions".
Colloid and Surfaces, 29, 411 (1988).

The University of Manchester Institute of Science and Technology
P.O. Box 88, Manchester M60 1QD, United Kingdom

A. S. Dunn

Telephone 061-236 3311
Telex 666094
Fax No 061-228 7040



Nicellar Polymerisation of Styrene

Chatterjee, Banerjee, & Konar (1979)
EMULSION POLYMERISATION OF
STYRENE at 50°C

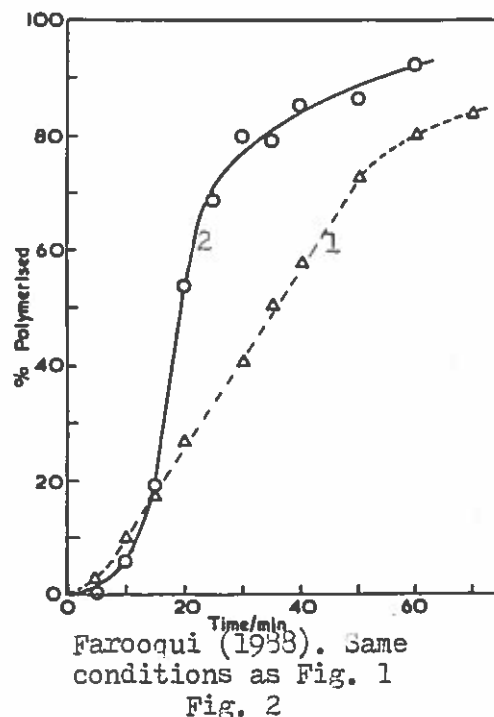
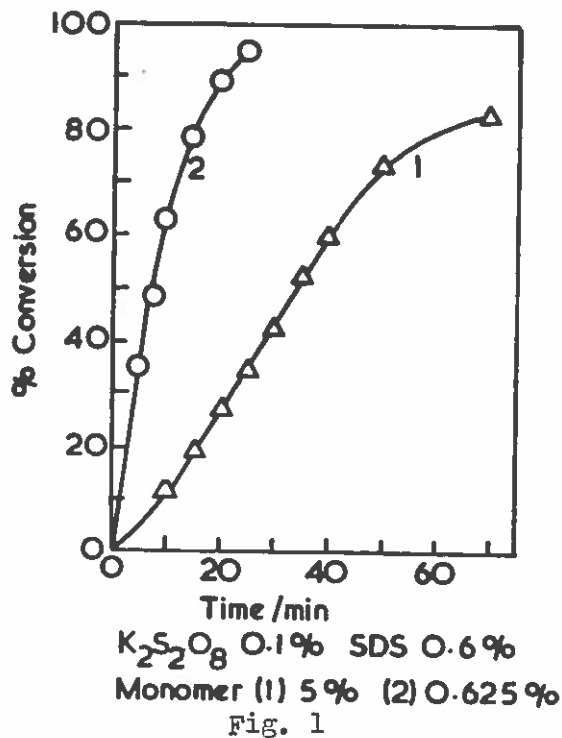


Fig. 1 is reproduced from *J. Polym. Sci. Polym. Chem. Edn.* 17 (1979) 2193 (7) (Curves A and D of the authors' Fig. 1). The authors only comment is incidental on the shape of Curve 2. Although the phase ratio is not generally a critical factor in emulsion polymerisation, the amount of monomer present under the conditions of Curve 2 is so low that it can all be solubilised in the emulsifier micelles i.e. there is no separate monomer phase. Consequently the monomer concentration at the locus of polymerisation cannot be constant at any stage of the polymerisation. Yet the rate does not decrease as would be expected in a first order reaction being substantially constant up to 55% at least in Curve 2 of Fig. 1. Dr Satpathy confirmed these observations when he was in Manchester. He reproduced Curve 1 exactly and also found that micellar styrene polymerised at a much faster rate than the 5% emulsion although not so fast as in Curve 2 of Fig. 1. The rate of the micellar polymerisation was sensitive to stirrer speed suggesting that stirring was inducing orthokinetic coalescence of latex particles.

Under somewhat different conditions Mishal, Litvinenko, Gritskova, Kaminskii, & Pravednikov (*Vysokomol. Soed. B* 25 (1933) 139 (2) - I can supply an English translation of this paper on request) also found a very high rate of polymerisation ($7\% \text{ min}^{-1}$) at low monomer contents: the rate was independent of phase ratio (1:100, 1:200) when persulphate initiation was used but the duration of Interval I depended on phase ratio when an oil-phase initiator - azodiisobutyronitrile - was used.

The obvious explanation of these results is that a larger number of latex particles is stabilised at the high emulsifier:monomer ratio in the micellar polymerisation experiments. However no particle size measurements were made in the experiments described above. Marie Farooqui has now measured the particle sizes of the completely polymerised latices using dynamic light scattering. This gives the hydrodynamic radius i.e. including any adsorbed layer. This is a \bar{z} -average if the latex is polydisperse. The index of polydispersity for the samples corresponds to $\bar{d}_w/\bar{d}_n = 1.5$ whence it can be inferred that $\bar{d}_w > \bar{d}_{mc}$ as required for calculating the particle number concentration N so that the absolute value of N calculated from \bar{d}_w will be low. However this error will not affect inferences from the relative values of N under the two conditions. For the 5% emulsion, $\bar{d}_w = 55.4$ nm which gives $N = 5.03 \times 10^{14}$ per cm^3 water. For the micellar case $\bar{d}_w = 35.3$ nm giving $N = 2.23 \times 10^{14}$ per cm^3 water because of the lower amount of monomer. However these are final particle numbers and it is possible that this results from extensive partial coalescence in the micellar case in view of the observed effect of stirring speed on the rate of polymerisation.

Reducing the surfactant concentration whilst keeping the styrene at 0.625% has the effect of reducing the duration of the 'Interval II' period during which the rate is at a maximum without changing the maximum rate observed i.e. the conversion at which the rate of latex particle coalescence begins to exceed the rate of latex particle nucleation is lower. The conversion at which this transition occurs at normal emulsifier:monomer ratios is probably too low to be observable.

Contribution to the Polymer Colloids Group Newsletter

M.S. El-Aasser, A. Klein, C.A. Silebi, J.W. Vanderhoff
E.S. Daniels, V.L. Dimonie, O.L. Shaffer, and E.D. Sudol

*Emulsion Polymers Institute, Lehigh University
Mountaintop Campus, Building A, 111 Research Drive
Bethlehem, Pennsylvania 18015-4732 U.S.A.*

The titles of our current research projects are given in the enclosed Contents of our Graduate Research Progress Reports, No. 29, January 1988. Copies of any of these reports can be obtained by contacting Ms. Debra Nyby at the above address. Summaries of recent progress in several research areas are presented here.

I. The Morphology of Microscopic Composite Particles Prepared by Two-Stage Polymerization (S. Shen)

The morphology of latex particles prepared by two-stage emulsion polymerization has been widely studied over the past decade. These studies have generally been limited to particles in the 100-500 nm diameter size range. Morphologies have ranged from true core-shell to fragmented and inverted core-shell structures. These are found to be influenced by the properties of the monomers and polymers, as well as the reaction conditions.

The study of the morphologies resulting from the preparation of microscopic polymer particles (diameter $> 1 \mu\text{m}$) was undertaken to investigate the effect of particle size on the resulting structure. These were prepared by a two-stage process comprising a dispersion polymerization to prepare the seed followed by seeded emulsion polymerization. Monodisperse polystyrene (PS) and poly(methyl methacrylate) (PMMA) particles produced by dispersion polymerization in ethanol and methanol, respectively, were cleaned and converted to aqueous dispersions. These were used as seeds in second-stage emulsion polymerizations in which styrene or methyl methacrylate monomer was added to the seed of opposite composition to give polystyrene-poly(methyl methacrylate) and poly(methyl methacrylate)-polystyrene composite particles.

These two types of composite particles showed different morphologies as shown through transmission electron microscope (TEM) examinations of microtomed sections and scanning electron microscope (SEM) examination of particles in which the poly(methyl methacrylate) was extracted by a suitable solvent mixture, leaving behind the insoluble polystyrene. Figure 1 depicts the respective morphologies found to be consistent with the two methods of examination. The PS-PMMA composite particles showed a smooth surface and a core-shell morphology with a PMMA shell and domains of PMMA present inside the PS core. However, the PMMA-PS composite particles appear to be somewhat more complex; PS domains were found to be present throughout the composite particles with those near the surface connected together by PS bridges. The surface of the particles appeared to consist of a thin PMMA layer. Further work is required to verify this.

MORPHOLOGY OF PS/PMMA

MORPHOLOGY OF PMMA/PS

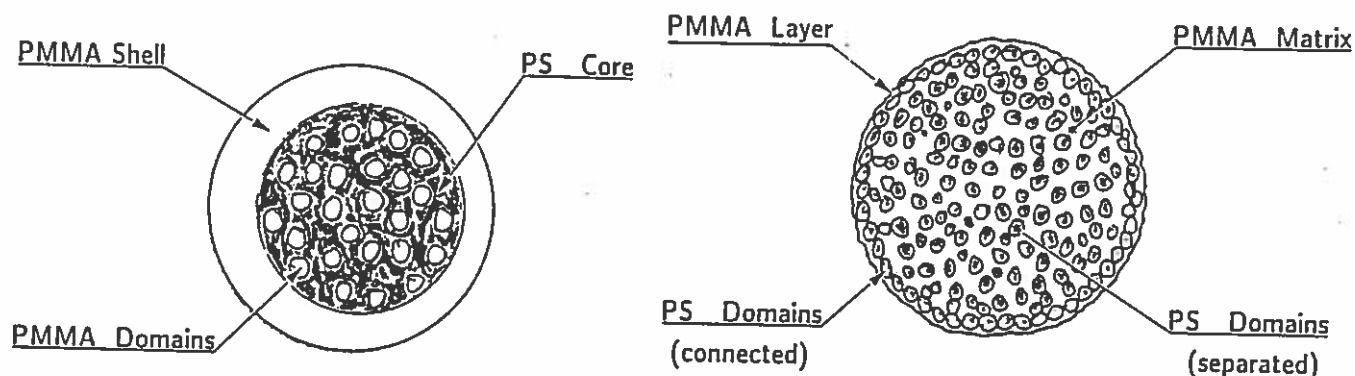


Figure 1. Schematic of the morphologies found for the polystyrene/poly(methyl methacrylate) and poly(methyl methacrylate)/polystyrene composite particles.

The extent of grafting, molecular weight analysis and further studies of the effect of reaction conditions on resulting morphology are planned.

II. Thin Layer Chromatography - Flame Ionization Detection Method for the Determination of Grafting (G. Levif)

The extent of grafting between Stage I (seed) and Stage II polymers plays an important role in determining the morphology of composite latex particles. The separation and characterization of the various constituents in polystyrene/poly(methyl methacrylate) composite latex particles, namely the graft copolymer and homopolymers, was undertaken using the thin layer chromatography/flame ionization detection (TLC-FID) technique. A 90/10 mixture (by volume) of toluene/methyl acetate was used as developer for the polystyrene fraction and acetonitrile for the poly(methyl methacrylate) fraction. These fractions were readily separated using successive developments. Separations were performed on Chromarods, used in the FID technique, as well as on conventional TLC plates. The latter was used to collect sufficient samples for infrared (FTIR) characterization of the constituents. For this technique to provide useful information, it was found that the seed latex used in the preparation must be free of any "impurities" which may not migrate with the PS or PMMA fractions and thus could be mistaken for graft copolymer. These could be polar (e.g. polymer with carbonyl end groups) or crosslinked materials. Nonetheless, this work suggests that the TLC/FID technique is a promising method for characterizing composite particles.

III. Emulsion Copolymerization of Poly(Butyl Acrylate-Co-Itaconic Acid) (M. Lock)

Carboxylated monomers are widely used in emulsion polymerization to improve the colloidal and mechanical stabilities of latexes. The dicarboxylated itaconic acid monomer has been used for these purposes; however, this functional monomer is difficult to copolymerize with conventional vinyl monomers. The presence of itaconic acid gave undesirable low conversion in the copolymerization with butyl acrylate where potassium persulfate was used as initiator. Furthermore, increasing the reaction temperature resulted in even lower conversions. This unconventional behavior was shown to be a consequence of a side reaction between itaconic acid and the potassium persulfate initiator used in the preparation of the latexes.

Potassium persulfate decomposition rate constants were determined under varying conditions and are given in Table 1. Note that only the presence of itaconic acid itself leads to great increases in the decomposition rate. Neither pH or chemically similar materials had significant effects on the decomposition rate. Apparently, the structure of itaconic acid, with an allylic methylene group situated next to a carboxylic acid, activates the methylene group to degradative hydrogen abstraction reactions with the persulfate radicals, which interferes with the proper function of the initiator. Improved conversions and more conventional behavior were found when 4,4'-azobis(4-cyanopentanoic acid) (ACPA) was used as the initiator for the emulsion copolymerization.

Table 1

K ₂ S ₂ O ₈ Decomposition Rate Constants [min ⁻¹ (x10 ⁴)]	
pH = 7.5, T = 50°C	1.07
pH = 2.5, T = 50°C	1.30
1% (76.9mM) Itaconic Acid (pH = 2.6, T = 50°C)	14.10
1% Itaconic Acid, T = 60°C	48.50
1% Itaconic Acid, T = 70°C	131.00
76.9 mM Malonic Acid, T = 50°C	1.85
76.9 mM Hydrogenated Itaconic Acid, T = 50°C	2.57

Abstracts of Papers to be Presented at the ACS Meeting,
Toronto, June 1988

Morphology and Characterization of Multiphase
Composite Latex Systems

E.S. Daniels, M.S. El-Aasser, A. Klein and J.W. Vanderhoff

A series of two- and three-stage composite latexes were prepared by sequential seeded emulsion polymerization. The Stage I poly(butyl acrylate-co-N-(iso-butoxymethyl) acrylamide) seed latex was crosslinked with varying proportions of ethylene glycol dimethacrylate. Stage II monomer consisted of styrene, an 80/20 styrene-acrylonitrile mixture, or methyl methacrylate. Stage III monomer was comprised primarily of butyl acrylate with a small fraction of N-(iso-butoxymethyl) acrylamide. A grafting/crosslinking monomer, allyl methacrylate, was employed to enhance interstage grafting and adhesion.

The morphology of the composite latex particles was found to depend on the degree of grafting between the polymer stages, the seed latex crosslinking level, Stage I polymer polarity and compatibility and Stage II monomer composition. Particle morphologies ranging from latex interpenetrating polymer networks (latex IPN's) to inverted composite structures were observed. Kinetic and grafting results showed that the composite latex particle surfaces were the main polymerization loci and the major sites for interstage grafting reactions.

Particle Morphology of the Composite Latexes Prepared By
Seeded Emulsion Polymerization

V.L. Dimonie, M.S. El-Aasser and J.W. Vanderhoff

Particle morphology of the multiple layered latexes prepared by seeded emulsion polymerization have been reported to vary widely from true "core-shell" structure to odd-shaped particles depending on the nature of the core and shell polymers.

The morphology of the polystyrene core/polyacrylate shell latex particles was studied as a function of the hydrophilicity of the second stage monomer, the polarity of the seed particle surface and the mode of monomer addition. The changes in the particle morphology were observed by Transmission Electron Microscopy using preferential staining of polystyrene domains with ruthenium tetroxide (RuO_4) combined with the negative staining with phosphotungstic acid (PTA). It was found that in addition to the viscosity of the polymerization locus, the interfacial tension of the polymer phases is the controlling parameter of the particle morphology in composite latexes.

Interparticle Monomer Transport in Miniemulsion Copolymerization

V.S. Rodriguez, M.S. El-Aasser, J. Delgado and C. Silebi

The mechanism of monomer transport in the miniemulsion copolymerization process is being studied. Theoretical predictions and experimental results

are presented on the monomer transport in the following case: a miniemulsion of monomer A is mixed with a miniemulsion of monomer B. The transport of A and B between the two types of droplets is studied and the effects of the type of cosurfactant used in the preparation of the miniemulsions, its concentration and transfer area are analyzed.

Two experimental approaches were developed to study different aspects of the monomer transport process. Styrene (St) and methyl methacrylate (MMA) were used as model monomers. The miniemulsions were prepared using sodium lauryl sulfate as surfactant and hexadecane or cetyl alcohol as cosurfactant.

The mechanism of transport and the effect of the cosurfactant type and concentration on the amount of monomer transported were studied in a compartmented diffusion cell. The cell consisted of two chambers divided by a semipermeable membrane. The membrane allows the passage of the molecular species but does not allow the passage of droplets or particles. The St-mini emulsion was placed in one of the chambers, and the MMA-mini emulsion containing the same or a different amount of cosurfactant was placed in the other chamber. The transport of the monomers from one chamber to the other was monitored by Gas Chromatography. The information rendered by the compartmented diffusion cell about the mechanism of transport and the effect of the cosurfactant on the transport process agreed with the predictions of the mathematical model. However, the high resistance of the membranes used, did not allow the determination of the mass transfer coefficients.

A second experimental approach was developed to determine the mass transfer coefficients of the monomers between the monomer droplets and the aqueous phase. The approach is based on the analysis of the composition of the copolymers formed by fast ultraviolet (UV) initiated polymerization of a mixture of the two miniemulsions and varying the mixing time period prior to the UV initiation.

Recent Publications

"The Miniemulsification Process - Different Form of Spontaneous Emulsification", M.S. El-Aasser, C.D. Lack, J.W. Vanderhoff and F.M. Fowkes, Colloids and Surfaces, 29, 103 (1988).

"Liquid Crystals in Dilute Mixed Emulsifier Sodium Lauryl Sulfate/Fatty Alcohol Solutions", C.D. Lack, M.S. El-Aasser, C.A. Silebi, J.W. Vanderhoff and F.M. Fowkes, Langmuir, 3, 1155 (1987).

Recent Ph.D. Dissertations and M.S. Theses

"Batch and Semi-Continuous Emulsion Polymerization of Vinylidene Chloride and n-Butyl Methacrylate", Ki-Chang Lee, Ph.D.

"Ultraviolet Light-Curing of Latex Films", Shigeo Hayashi, M.S.

"Film Properties of Carboxylated Latexes", Eisuke Natsuhara, M.S.

"Batch and Semicontinuous Copolymerization of Vinyl Acetate and Methyl Acrylate", Hope Pelsynski, M.S.

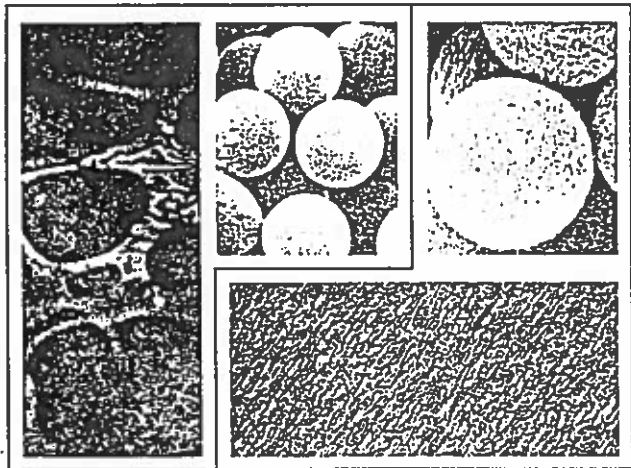
"Polymerization of Styrene Microemulsion", Jong-Shing Guo, M.S.

Copies of the abstracts are available upon request.

The Emulsion Polymers Institute's 19th Annual Short Course "Advances in Emulsion Polymerization and Latex Technology" will be held at Lehigh on June 6-10, 1988. The European Short Course will be given August 22-26, 1988.

EMULSION POLYMERS INSTITUTE

Graduate Research Progress Reports No. 29
January 1988



Lehigh University



Bethlehem, Pennsylvania

CONTENTS

	Page
Emulsion Polymers Institute - Staff	1
PREPARATION OF POLYMER COLLOIDS	
Preparation, Swelling and Phase Separation of Large-Particle-Size Monodisperse Latexes (H.R. Shou, M.S. El-Aasser and J.V. Vanderhoff)	6
Preparation of Uniform Polymer Particles by Dispersion Polymerization in Organic Media (Y.Y. Lu, M.S. El-Aasser and J.V. Vanderhoff)	16
The Morphology of Large Composite Particles Prepared by Two-Stage Polymerization (S. Shen, V.L. Dismone, M.S. El-Aasser and J.V. Vanderhoff)	28
Liquid Crystalline Behavior of Aqueous Sodium Dodecyl Sulfate and Cetyl Alcohol Mixed Emulsifier Systems (R. Coetz, J. Delgado, M.S. El-Aasser, F.H. Fouke, Y. Kim and J.V. Vanderhoff)	35
Interparticle Monomer Transport in Miniemulsion Copolymerization (V.S. Rodriguez, J. Delgado, M.S. El-Aasser and J.V. Vanderhoff)	43
Batch and Semicontinuous Copolymerization of Vinyl Acetate and Methyl Acrylate (M.A. Pelsynski, J. Delgado, M.S. El-Aasser and J.V. Vanderhoff)	53
Polymerization of Styrene Microemulsions (J.S. Guo, M.S. El-Aasser and J.V. Vanderhoff)	55
Grafting Reactions of Poly(vinyl Alcohol) during the Emulsion Copolymerization of Vinyl Acetate and Butyl Acrylate (M.J. Earhart, V. Dismone, M.S. El-Aasser and J.V. Vanderhoff)	59
Preparation and Characterization of Vinylidene Chloride (VDC)/n-Butyl Methacrylate (BMA) Core/Shell Latexes by Batch and Semicontinuous Emulsion Polymerization (M.M.H. Ayoub, M.S. El-Aasser and J.V. Vanderhoff)	66
Preparation and Characterization of Acrylate Latexes Containing Dicarboxylic Acid Comonomers (M. Lock, M.S. El-Aasser and J.V. Vanderhoff)	70
Film Properties of Carboxylated Latexes (E. Natsuhara, J.V. Vanderhoff and M.S. El-Aasser)	79

CHARACTERIZATION OF POLYMER COLLOIDS

Some Aspects of Polymer Separation Using the TLC-FID Method (C. Leviz, V.L. Dismone, M.S. El-Aasser and J.V. Vanderhoff)	81
Morphology of a Soft Latex (O. Shaffer, M.S. El-Aasser, A. Klein and J.V. Vanderhoff)	89
The Role of Avanel 5 Surfactants in Emulsion Polymerization (E.S. Daniels, M.S. El-Aasser and J.V. Vanderhoff)	97
Comparative Effects of Alkyl Chain Length and Degree of Substitution on the Adsorption of Dowfax™ Emulsifiers at the Monomer/Water Interface (V.L. Dismone, M.S. El-Aasser and J.V. Vanderhoff)	111

POLYMERIZATION REACTOR DESIGN AND CONTROL

Modeling and Control of Semicontinuous Emulsion Copolymerization (J. Dismone, C. Georgakis, M.S. El-Aasser and A. Klein)	119
Inverse Emulsion Polymerization of Acrylamide in a Tubular Reactor (T.F. Bash, M.S. El-Aasser and J.V. Vanderhoff)	136
Continuous Miniemulsion Copolymerization of Vinyl Acetate and n-Butyl Acrylate in a Tubular Reactor (S. Adamec, J. Delgado, M.S. El-Aasser and J.V. Vanderhoff)	155

APPLICATIONS OF POLYMER COLLOIDS

Preparation of Rocket Propellants by Emulsification (T.V. Hawkins, M.S. El-Aasser and J.V. Vanderhoff)	158
U.V. Curing of Latex Films (S. Hayashi, M.S. El-Aasser and J.V. Vanderhoff)	167
Preparation of Water-Absorbent Polymers by Inverse Suspension Polymerization (Y.S. Chang, V.L. Dismone, M.S. El-Aasser and J.V. Vanderhoff)	168
Coagulation Studies of Solvent-Swollen Latex Particles in a Stirred Tank Reactor (J. Uydila and A. Klein)	173

Associative Thickeners: An Investigation Into Their Thickening Mechanism (R. Jenkins, C.A. Silabi, M.S. El-Aasser and J.V. Vanderhoff)	184
--	-----

Hollow Polymer Particles: Preparation, Characterization and Application (J.M. Park, J.V. Vanderhoff and M.S. El-Aasser)	203
---	-----

DISSERTATION AND THESIS TITLES	214
---------------------------------------	------------

ON THE PROPERTIES AND MICROSTRUCTURE OF COMPOSITE LATEX POLYMERS

Eliseeva V.I. and Titova N.V.

Earlier it was shown that in semicontinuous polymerization of acrylic monomers on PMMA seed latex, in the conditions when a thermodynamically equilibrium swelling of the seed particles in the monomer is not reached, a new fraction of particles is formed; as they appear these particles flocculate with the particles of the seed latex /1/. It was also established that with incomplete conversion of the seed latex monomer the particles of the final latex consist of two segregated polymers of the first and the second stages and a copolymer of intermediate chemical composition, playing the part of a transition layer. Removal of this layer from the phase boundary results in a substantial decrease in the strength of the polymer (film extracted from the latex. This transition layer is thus of great significance for the polymer properties. Up to now, however, its structure and formation mechanism have not been properly ascertained.

The present work was devoted to investigating the influence exerted by the conversion of the PMMA seed latex monomer, when a mixture of butyl acrylate (BA) with methacrylic acid (MAA) is polymerized in its presence, on the mechanical behaviour of latex films and the transition layer structure. This was of special interest in connection with the works that have appeared, dealing with accelerated seed polymerization on particles with incomplete monomer conversion (shot - growth) /2/, leading to the formation of films with enhanced strength. It was assumed that the content of "their own" monomer absorbed by the seed particles, as well as of the monomers introduced at the second stage, must influence both the transition layer structure and the nature of its interaction with the seed particles.

Five latexes of a given monomeric composition were synthesized by means of BA-MAA (90-10) seed polymerization on PMMA latex with a differing monomer conversion.

From the synthesized latexes films were obtained by drying on glass in room conditions, followed by vacuum drying in a desiccator for 5-6 days (pressure 10^{-1} mm merc.). Mechanical properties of the films (0.2 mm thick) were characterized by the stress-strain curves obtained on a Poliani instrument with automatic recording. The maximum relative error of the arithmetic mean of 10 measurements for a 0.95 confidence level amounted to 10%.

The transition layer structure was identified by a change in the stereostructures of PMMA macromolecules (cores of particles), occurring in the course of seed polymerization, with the help of ^{13}C NMR spectroscopy.

Figure 1 shows the stress-strain curves for the films obtained from latexes. Mechanical behaviour of the films is seen to differ sharply, depending on the seed latex monomer conversion: with an increase in conversion from 72 to 100% the elongation increases from 50 to 550%, and the ultimate tensile stress - from 10 to 16 MPa.

As already noted, in semicontinuous seed polymerization of such monomers new particles of a second polymer are formed /1/; the monomer introduced at the second stage is thus absorbed by both the new and the seed particles. It has been suggested that the fraction of the second monomer absorbed by the seed particles is copolymerized with the residual monomer contained in them, which leads to the formation of a copolymer of intermediate chemical composition /3/. However, this copolymer could be formed both as a result of statistical copolymerization alone and by the formed macromolecules being grafted to the seed latex polymer. Judging by the shape of the stress-strain curves at low conversion values (72%), a statistical copolymer

in considerable quantities is predominantly formed. On the other hand judging by the curves for films from the latexes obtained at a high conversion of seed latex monomer (curves 3,4,5, Fig.1), predominant in the second stage of polymerization is the grafting of copolymer II (BA-MAA) on the polymer of the cores of particles (PMMA): an increase in elasticity can be explained by the elastic matrix, formed from the "shells" of particles, responding to the applied stress. Moreover, at 100% conversion of the seed latex monomer only the grafting is possible (curve 5, Fig.1).

This view was confirmed with the help of the data of ^{13}C NMR spectra, obtained when investigating the samples of the corresponding latex films. Figure 2 shows a fragment of the ^{13}C $\{^1\text{H}\}$ NMR spectrum for a sample of latex 3. The signals in the spectrum were assigned on the strength of the data from /4 - 7/. Clearly seen in the spectrum are the signals from the triads in PMMA: syndio - s, hetero - h, isotactic - i sequences (CCH_3 , quat.C).

The values of integral intensities of the signals from triadic stereosequences in PMMA were used to determine the microtacticity of PMMA seed latex and of PMMA in the composite polymers of latexes 1-4.

Figure 3 shows the molar fractions of rr(s), mm(i) and rm+mr(h) triads in the corresponding samples. Also shown there are the values of isotacticity coefficient P_m . It is seen that the largest deviations of microtacticity from the initial seed latex polymer (isolated points in Fig.3) are observed in the samples obtained with the highest conversion of the seed latex monomer (mm(i), rr(s)). The value of the isotacticity coefficient P_m also decreases, the higher the seed latex conversion the greater the decrease; in sample 4 (97% conversion) it decreases 1.3 times in comparison with the initial polymer. These changes in PMMA microstructure can only be associated with a

change in the configuration of the units of macromolecules in the core of particles as a result of copolymers II (MMA-BA-MAA) or II (BA-MAA) being grafted to them.

From the data obtained a conclusion can be drawn that the formation of a graft copolymer in the course of seed polymerization is the more pronounced the higher the seed latex monomer conversion. And, vice versa, a decrease in its conversion leads to an increase in the fraction (in the transition layer) of the statistical copolymer whose formation does not cause any change in the configuration of seed latex macromolecules.

This conclusion is confirmed by the analysis of mechanical behaviour of the corresponding films (Fig.1): an increase in elongation with an increase in the elastic polymer grafting to the rigid core and a decrease in elongation with an increase of the statistical copolymer content in the transition layer. The structure of the particles formed in both cases can be schematically presented as shown in Figure 4, which explains the difference in the mechanical properties of films.

From the data presented in this communication it follows that ^{13}C NMR analysis of the microstructure of copolymers obtained by means of seed polymerization makes it possible to discern the fine features of the process taking place at the "core" - "shell" interface and to explain the difference in the mechanical properties of the polymer, depending on the structure of the transition layer in composite particles.

References

1. Eliseeva V.I., Gerasimova A.S., Frantsuz Z.S., Titova N.V., Afanasyeva N.V., Borisova T.I., Vysokomolek. soed., 1984, A, v.26, N°7, p.1382.
2. Chainey M., Wilkinson M.C., Hearn J., Ind. Eng. Chem. Prod. Res. Dev., 1983, v.21, N°2, p.171.
3. Afanasyeva N.V., Borisova T.I., Chichagova E.R., Shevelov V.A., Titova N.V., Eliseeva V.I., Vysokomolek. soyed, 1982, A, v.24, N°5, p.1027.
4. Ivin K.J., Pitchumani S., Reddy C.R., Rajaduarai S., Europ. Polym. J., 1981, v.17, p.341.
5. Niknam M.K., Majumdar R.N., Blouin F.A., Harwood H., Macromol. Chem., Rapid Commun., 1982, v.3, p.825.
6. Pham Q.-F., Trends in Anal. Chem., 1983, v.2, N°3, p.67.
7. Ferguson R.C., Ovenall D.W., Amer. Chem. Soc., Polym. Prepr., 1985, v.26, N°1, p.182.

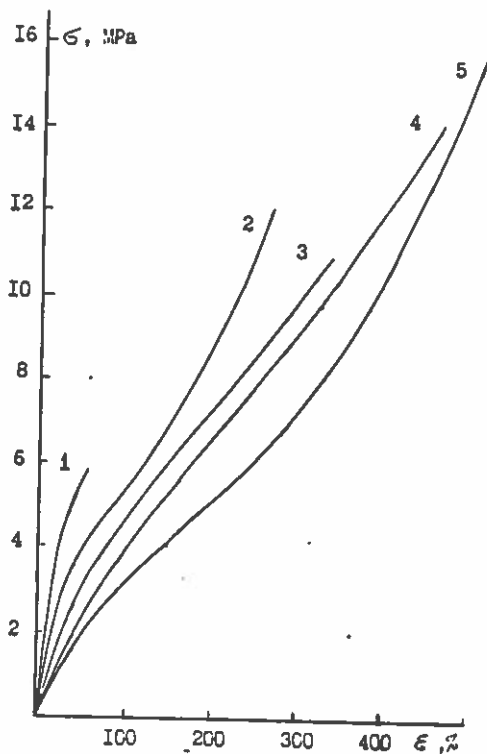


Fig.1 Stress-strain curves for films from latexes 1(1),2(2),3(3),4(4),5(5), (seed latex monomer conversion 72,82, 90,97,100%,respectively).

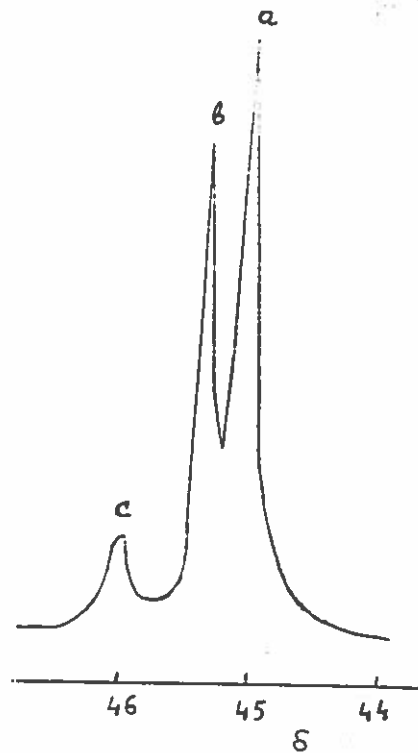


Fig.2 Fragment of $^{13}\text{C}\{^1\text{H}\}$ NMR spectrum for 25 wt.% solution in DMSO-D_6 of the film from latex 3. Chemical shifts are given with respect to TMS. Assignment of signals - quat.C: a-rr(s),b-mr(h), c-mm(i).

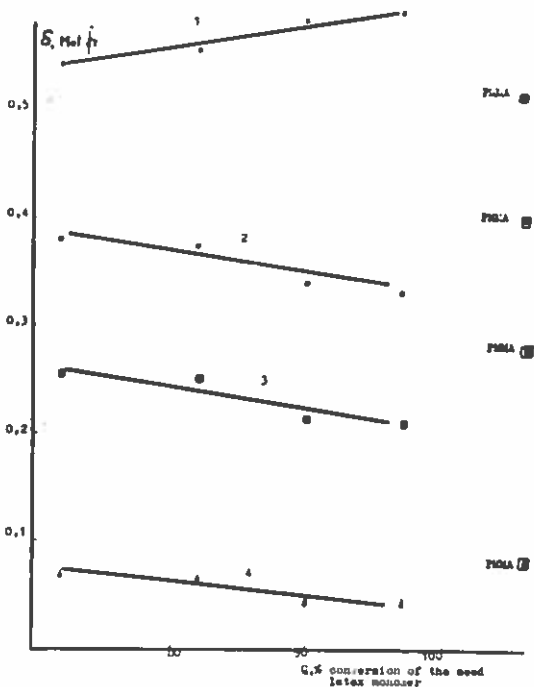


Fig.3 PMMA microtacticity in the core and the composite polymer, depending on MMA conversion: 1-rr(s), 2-rm+mr(h), 3- P_m , 4-mm(i).

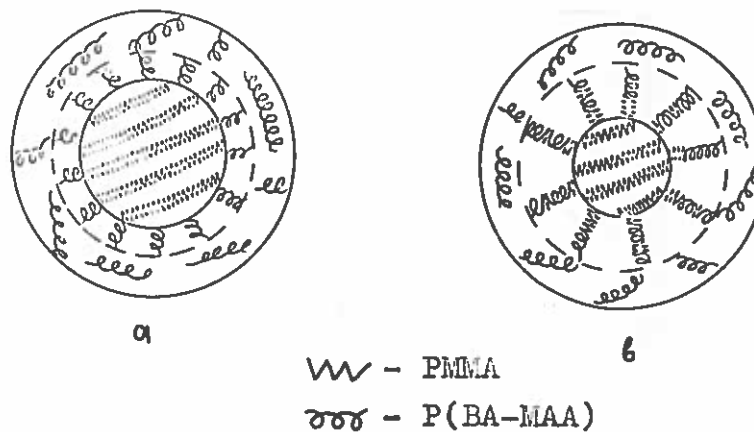


Fig.4 Schematic structures of particles of latexes obtained at: a - incomplete (latex 1) b - high (latexes 4,5) conversion of seed latex monomer

ON THE STRUCTURE OF LATEX FILMS

V.I.Eliseeva, V.N.Cherniy

Institute of Physical Chemistry, USSR Academy of Sciences

The present research was undertaken with the aim of quantitative determination of the content and the distribution of the emulsifier in the films obtained by drying of latex in air and electrodeposition of polymer from latex on the metal anode.

Radioisotope method has been used for this purpose: the latex synthesis was carried out at a constant concentration of sodium dodecylsulfate labelled with S^{35} (2% from the sum of the monomers). The change in radioactivity of the film in the course of its formation and keeping in water allowed to determine the content of emulsifier and its distribution in the film. Latex copolymers of MMA and ST with BA in different ratio (i.e. polymers with different T_g) were used. The initiator (ammonium persulfate) concentration for all the latexes was constant.

It has been assumed that the total emulsifier content in the film obtained by the drying of the latex is determined by the concentration of the emulsifier in the corresponding volume of latex and was taken for 100%. The change in the emulsifier content in the course of electrodeposition of the MMA-BA copolymers with different T_g on the copper anode is shown in Fig.1a,b. It is evident that if the T_g of the polymer is lower than the ambient temperature ($+14^\circ C$) the emulsifier content in the electrodeposit is somewhat lowered (curve 2a) whereas in case of the polymers with T_g higher than ambient temperature ($+28^\circ C$) the emulsifier content in the electrodeposit increases. In the first case dense layers are formed which lead to isolation of anode and creation of better conditions for electroosmosis, in the second case the layers formed are porous with conducting channels filled with electrolyte, such deposits contain more discrete particles stabilized by the emulsifier. This explanation is supported by the fact that the rate of the change of the strength of current in the first case is greater (curve 3a) than in the second case (curve 3b) and by the kinetics of accumulation of the polymer in the electrophoretic deposits (curves 1a,b).

The change of the emulsifier content in the film in the course of its keeping in water was regarded as a measure of the strength of its bonding in the film. The experimental data presented in Fig.2 suggest two types of bonding of the emulsifier in the films: one part of the emulsifier bonded weaker is eliminated for 10-12 days, the remaining most part of the emulsifier cannot be eliminated from the film even after following 50 days of keeping in water. The completion of the emulsifier leaching correlates with the time necessary to achieve the equilibria swelling of films in water (which comes to 10-12 days as well). The inflections of kinetic curves are more pronounced for the latex films obtained by electrodeposition than for the films obtained by the drying of latex in air, however the ultimate emulsifier content in the latter is lower. The equilibria emulsifier content is higher for the more hydrophobic tough polymers, no correlation with the value of the equilibria swelling in water being observed.

All the data obtained may be explained if the structure of latex film is regarded as a polymer matrix threaded by capillary network. The emulsifier is distributed between the capillaries and the matrix. The first (capillary) part of the emulsifier can be easily leached when the film is plunged in water, whereas the contact of water with the second (matrix) part of the emulsifier and its leaching depends on hydrophilicity and mobility of the polymer chains, the latter increasing with the increase of polarity and decrease of T_g of the polymer.

Fig. 1 Kinetics of the formation of the layer during electrodeposition of the polymers with $T_s = 14^\circ\text{C}$ (a) and $T_s = 28^\circ\text{C}$ (b) on the copper anode from the MMA-BA latex.

1 - mass of the polymer (m);
 2 - emulsifier concentration (c);
 3 - current strength (j);
 4 - water concentration (w)

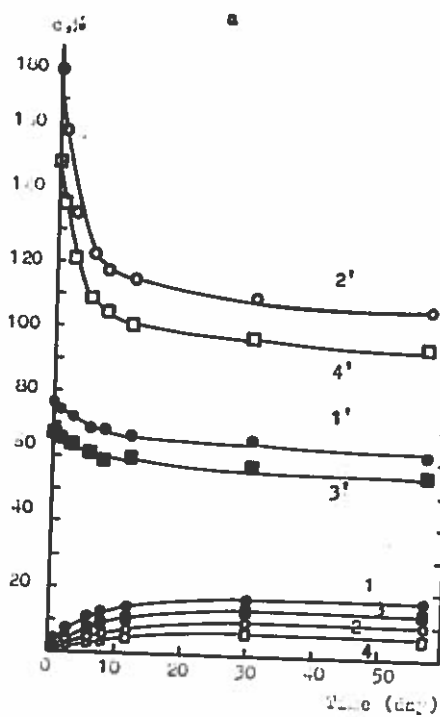
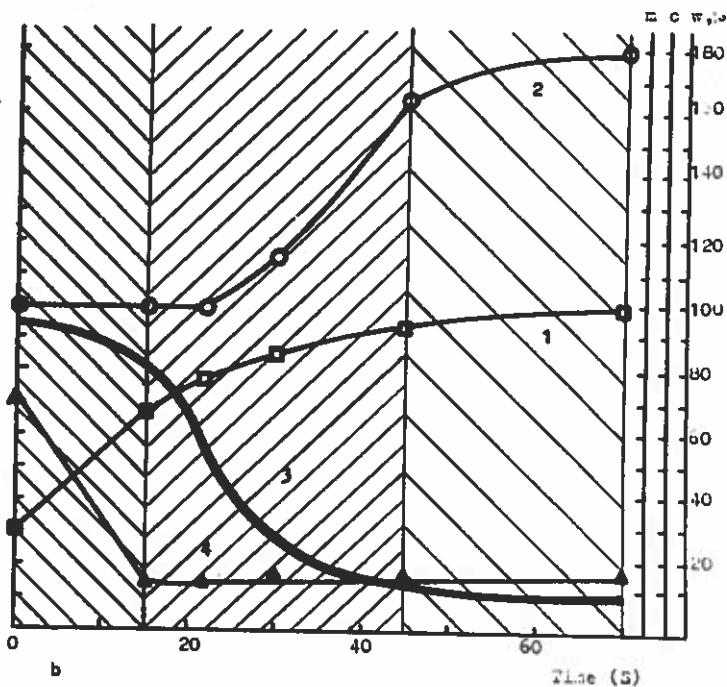
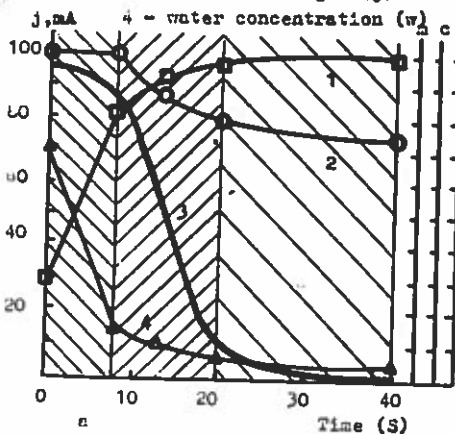
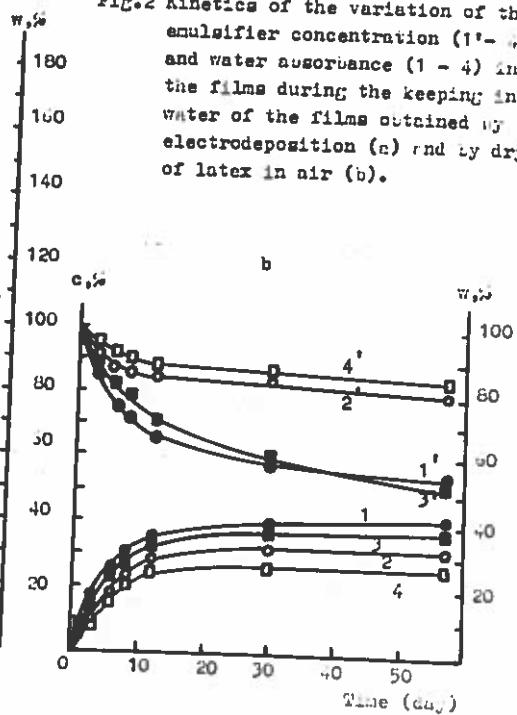


Fig. 2 Kinetics of the variation of the emulsifier concentration (1' - 4') and water absorbance (1 - 4) in the films during the keeping in water of the films obtained by electrodeposition (a) and by drying of latex in air (b).



DEPARTMENT OF CHEMICAL ENGINEERING

Contribution to Polymer Colloids Newsletter
Current Research Projects - Alice P. Gast
April 1988

1. Fluorescence Studies of Polymer Adsorption:
Rearrangement and Displacement of Pyrene-terminated Poly(ethylene glycol)
on Colloidal Silica Particles
with Kookheon Char (jointly advised with C. W. Frank)

Goal: To understand the conformational behavior of polymer chains confined to colloidal surfaces as a function of surface chemistry, surface curvature and polymer solution thermodynamics.

Summary: Adsorption of pyrene end-labeled poly(ethylene glycols) (Py-PEG-Py) on colloidal silica particles and their subsequent rearrangement and/or displacement by the addition of unlabeled PEG are studied in water using photostationary fluorescence and time-resolved fluorescence decay. The tagged polymers we use in this study have molecular weights 4250 and 8650 based on the PEG backbone. The molecular weight of the displacing polymer (PEG) ranges from 1470 to 22000. Experimental conditions for the adsorption of Py-PEG-Py are chosen to ensure that a negligible amount of Py-PEG-Py exists in free solution. For the adsorption of Py-PEG-Py (8650) of 1×10^{-6} M on silica particles at 0.1 wt % concentration there is an overshoot in the excimer to monomer intensity ratio, I_e/I_m , relative to that of bulk solution, $(I_e/I_m)_0$, as the displacer (PEG (22000)) concentration is increased. This overshoot is not detected for the adsorption of Py-PEG-Py (4250). Analysis of the supernatant solution shows that the overshoot may be attributed to the rearrangement of Py-PEG-Py (8650) on the silica surface due to the adsorption of incoming displacer prior to displacement of the tagged PEG into solution. We speculate that there is a competition between rearrangement of Py-PEG-Py on the surface and displacement into bulk solution that depends upon the absolute number of Py-PEG-Py segments actually in contact with the surface. The effects of the molecular weight of the displacing polymer and the initial concentration of Py-PEG-Py on $(I_e/I_m)/(I_e/I_m)_0$ are also studied. The measurement of excitation spectra and time-resolved fluorescence decays for both monomer and excimer emission provides insight into the state of the Py-PEG-Py when adsorbed on the surface.

We are currently developing a theory for the system described above using an equation similar to the self-consistent field equation of Edwards and comparison between experiment and theory will be made.

Publication accepted in Langmuir.

2. Thermodynamic and Kinetic Studies of Charged Colloidal Suspensions
with Yiannis Monovoukas

Goal: To determine the mechanisms of nucleation and growth of volume-filling entropically driven crystals of a model colloidal suspension.

Summary: Suspensions of charged colloidal particles are ideal for model studies of crystallization because they are easily observed with optical techniques and their forces are readily manipulated by controlling the chemistry of the suspension medium. We studied the order-disorder and BCC-FCC transitions of a model suspension of highly charged polystyrene spheres as a function of the particle volume fraction and the ionic strength. We analyzed Kossel lines, produced by backscattered light diffraction, to identify the crystal structures and determine the interparticle spacings. Our results include a phase diagram showing that the BCC structure is stable at ionic strengths lower than 2.7×10^{-6} M KCl and volume fractions less than 0.008, whereas the

FCC structure is stable at higher volume fractions. We compared our experimental phase diagram with analytical models and recent molecular dynamics (MD) simulations. Existing analytical models predicting the BCC-FCC boundary are in clear disagreement with both the MD results and our data. Using an effective particle charge density, we found a very good agreement between our experimental results and the MD predictions for both the solid-liquid and solid-solid transitions.

We are currently investigating the rate of two-dimensional crystal growth and the concentration profile between crystalline and disordered regions that we will compare with theoretical predictions.

Publication submitted to Journal of Colloid and Interface Science.

3. A Microscopic Model of Electrorheology with Paul M. Adriani

Goal: To model the structure and resulting macroscopic properties of suspensions in external fields.

Summary: We model an electrorheological fluid as a concentrated suspension of hard spheres with aligned field-induced electric dipole moments. The presence of dipole moments causes clustering of the particles into an anisotropic suspension characterized by a particle probability distribution function. For strong external fields we predict via mean field theory a phase transition to particle-rich and particle-poor phases. We calculate the high frequency elastic shear modulus and the dynamic viscosity for each phase and then calculate the overall rheological response. We find the elastic shear modulus and the dynamic viscosity as a function of electric field strength. In the single phase region the dynamic viscosity is insensitive to field strength, but in the two phase region the dynamic viscosity increases with field strength since the particle concentration in each phase varies with field strength. In the single phase region the elastic shear modulus increases strongly with field strength, indicating sensitivity of elastic properties to the particle distribution. In the two phase region the elastic shear modulus increases very strongly, due to the changing particle concentrations and particle distribution. The results of these calculations provide insight into how microscopic structural changes affect the macroscopic properties of an electrorheological fluid.

Publication submitted to Physics of Fluids.

THE COPOLYMERIZATION OF CATIONIC MONOMERS WITH ACRYLAMIDE
IN SOLUTION AND INVERSE-MICROSUSPENSION

D. Hunkeler, A.E. Hamielec and W. Baade

Institute for Polymer Production Technology,

Department of Chemical Engineering,

McMaster University, Hamilton, Ontario, Canada L8S 4L7

(416) 523-1643

The free radical copolymerization of acrylamide with three of the most commonly used cationic comonomers diallyldimethylammonium chloride, dimethylaminoethylmethacrylate, and dimethylaminoethylacrylate, the latter two quaternized with methyl chloride, was investigated. The polymerizations were carried out in solution and inverse-microsuspension with azocyanovaleic acid and potassium persulphate over the temperature range, 45 to 60°C. The copolymer reactivity ratios were determined with error-in-variables method using residual monomer concentrations. These residual monomer concentrations were measured by a HPLC method which shows a considerably larger accuracy than colloid titration which has been commonly used in the past. The monomer partitioning between the aqueous and organic phases was measured in the presence of different levels of emulsifier.

Keywords: acrylamide, diallyldimethylammonium chloride, dimethylaminoethylmethacrylate, dimethylaminoethylacrylate, inverse emulsion, inverse micro-suspension, water soluble polymers.

MECHANISM, KINETICS AND MODELLING OF THE INVERSE-
MICROSUSPENSION HOMOPOLYMERIZATION
OF ACRYLAMIDE

D. Hunkeler, A.E. Hamielec and W. Baade

ABSTRACT

The polymerization of water soluble monomers is industrially most often carried out in inverse-microsuspension or inverse-emulsion. Although the kinetics of these processes have been investigated extensively over the past decade, there has been no mechanism proposed which can predict rates and molecular weights. In this paper a general mechanism is developed for inverse-microsuspension polymerization in paraffinic media with oil soluble initiators. It is compared with experimental data for acrylamide polymerizations and is found to predict conversion, molecular weight and particle characteristics quite well. The mechanism consists of the initiation, propagation, transfer and termination reactions that are common to all free radical polymerizations. It also includes three newly proposed steps: the reaction between a macroradical and an interfacial emulsifier, which has been found to dominate over the conventional bimolecular reaction, a long chain branching reaction with terminal unsaturated carbons, and the mass transfer of primary and oligo radicals between organic and aqueous phases. These have a profound effect on the kinetics, where the rate is found to depend on the initiator level to a power greater than one half, and is inversely proportional to the surface emulsifier concentration.

Due to the importance of unimolecular termination and long chain branching in inverse-microsuspension certain classes of emulsifier have been identified as being most suitable for the production of ultra high molecular weight polymers.

PRODUCTION OF SOAP - FREE AND SEED PARTICLES
OF POLYVINYLACETATE LATEX

N. Ali & A. E. Hamielec

McMaster Institute for Polymer Production Technology
McMaster University
Hamilton, Ontario, Canada L8S 4L7
Phone: (416) 523 - 1643

ABSTRACT

The production of polyvinylacetate latex in absence of surfactant (soap - free) has been carried out at 65° c , in a bench - scale reactor (500 ml) . Ammonium persulfate was used as an initiator . The effects of initial monomer concentration on the number of polymer particles , particle size and particle size distribution (PSD) of the latex produced have been studied . It was shown that a monodisperse particle size distribution could be obtained . The number of polymer particles per liter (N_p) decreases with monomer conversion and N_p is proportional to the initial monomer concentration to the - 1.5 power . The variation of the particle diameter and the number of particles per liter was also investigated soap - free seed particles . It was shown that a monodispersed distribution could be obtained and N_p decreased slowly with conversion .

SUSPENSION POLYMERIZATION OF VINYL CHLORIDE AT HIGH CONVERSION, MODELLING CONVERSION AND TRACER RESPONSE BY GAS CHROMATOGRAPHY. T.Y. Xie, A.E. Hamielec, P.E. Wood and D.R. Woods, Institute for Polymer Production Technology, McMaster University, Hamilton, Ontario, Canada, L8S 4L7.

A model for suspension polymerization relating the conversion of vinyl chloride (VCM) and the tracer response by online gas chromatography was developed. This model can be used to calculate VCM conversions using polymerization conditions and tracer responses over the entire conversion range. The distributions of both tracer and monomer in the different phases of the suspension polymerization system were considered in the model development. A series of experiments for suspension polymerization of vinyl chloride using n-butane as a tracer were carried out to evaluate the model. The distribution of tracer in the water, monomer, polymer and head space was evaluated according to the experimental results. The online gas chromatography can automatically sample every six minutes under the present experimental conditions. This technique can be used to study the kinetics of polymerization of vinyl chloride and hopefully to monitor the polymerization processes on an industrial scale.

SMALL ANGLE NEUTRON SCATTERING (SANS) STUDIES
ON CONCENTRATED POLYSTYRENE DISPERSIONS

D. S. Jayasuriya (S. C. Johnson & Son, Inc., Racine, WI)

and

P. Thiyagarajan (Argonne National Laboratory, Argonne, IL)

Abstract

Two series of experiments were carried out using a sulfated polystyrene latex with an average particle diameter of 38 nm and a surface charge density of $0.57 \mu\text{Ccm}^{-2}$ (corresponds to 162 SO_4^- per particle). Dispersions were made in deuterated water [88% D_2O (v/v)].

In the first series, scattered intensity profiles, $I(Q)$ were measured for the latex dispersions having particle volume fractions between 0.0075 and 0.074. The added electrolyte concentration in the medium was varied from 0 to 0.01 M using NaCl. Absolute $I(Q)$ profiles were fitted to a model based on a generalized macroion (GOCM) theory to evaluate average particle diameter with its polydispersity index and the effective surface charge ^{1,2}. (Polydispersity index is defined as the ratio of the standard deviation in diameter to the average diameter). In fitting the data, the contribution to the ionic strength due to the counter ions of the surface sulfate groups has been taken into account. For the dispersions with no added salt, the agreement between the theory and experiment is good, as shown in Fig. 1. The fitted particle diameters and polydispersity index agree well with electron microscopy data (Table 1). However, the fitted surface charges are about 25% of the values obtained from conductometry. GOCM theory gave poor

fits to the data on the systems with added electrolytes presumably due to the exclusion of the van der Waals attraction in the theory. Hence, the data are being analyzed on the basis of an effective hard sphere model where a more realistic inter-particle interaction could be used³.

The second experiment was carried out to study the effect of changing polyethylene oxide (PEO) concentration on the inter-particle interaction of charged latex particles. Latex dispersions with a fixed particle volume fraction of 0.034 in the presence of PEO (Mw=19.6K and 3.4K) in the concentration range of 0.05% to 5% (w/v) were used. As a first approximation, assuming that PEO only affects the effective surface charge, $I(Q)$ profiles were fitted to a model based on GOCM theory. The poor fits obtained indicate the inadequacy of this treatment. The mean inter-particle distances calculated from the maxima in $I(Q)$ on the basis of Bragg condition shows a minimum at PEO concentration of 2.5% for both molecular weights. These results for the PEO (Mw=19.6K) are presented in Fig. 2 along with the zeta-potential data. The difference in the trends between the two variables shows the importance of effects other than ionic double layer repulsion in the systems containing dissolved polymer. Although more data at other PEO concentrations are needed for verification, the trends observed in the inter-particle distances agree well with the flocculation behavior observed for charged colloids in the presence of dissolved polymer⁴. In spite of its obvious practical importance, very little is understood about this phenomenon. Computer programs are being developed to analyze the data using models which take into account both the steric stabilization and the polymer osmotic effects.

Acknowledgement

This work has benefited from the use of the Intense Pulsed Neutron Source at Argonne National Laboratory funded by the U. S. Department of Energy (contract W-31-109-Eng-38).

References

1. Wu, C. F. & Chen, S. H., J. Chem. Phys. 87, 6199 (1987).
2. Jayasuriya, D. S., Tcheurekdjian, N., Wu, C. F., Chen, S. H., and Thiyagarajan, P., J. Appl. Cryst. (1988) (In press).
3. Cebula, D. J., Goodwin, J. W., Jeffrey, C. G., Ottewill, R. H., Prentich, A. and Richardson, R. A., J. Chem. Soc., Faraday Trans. 1. 76, 1 (1983).
4. Cowell, C. and Vincent, B. in "The Effect of Polymers on Dispersion Properties, Th. F. Tadros (Ed.), Academic Press, (New York), 263 (1983).

Table 1

Sample	ϕ	Diameter (A)	p%	Z
A1	0.0741	361		37
A2	0.0556	366		37
A3	0.0371	367	9.95	36
A4	0.0185	364		36
A5	0.0093	359		21

Note: Average particle diameter = 380 A (EM)
Polydispersity ratio = 9.95 (EM)
Charges per particle (Z) = 162 (Conductometry)

ϕ = particle volume fraction

Figure 1

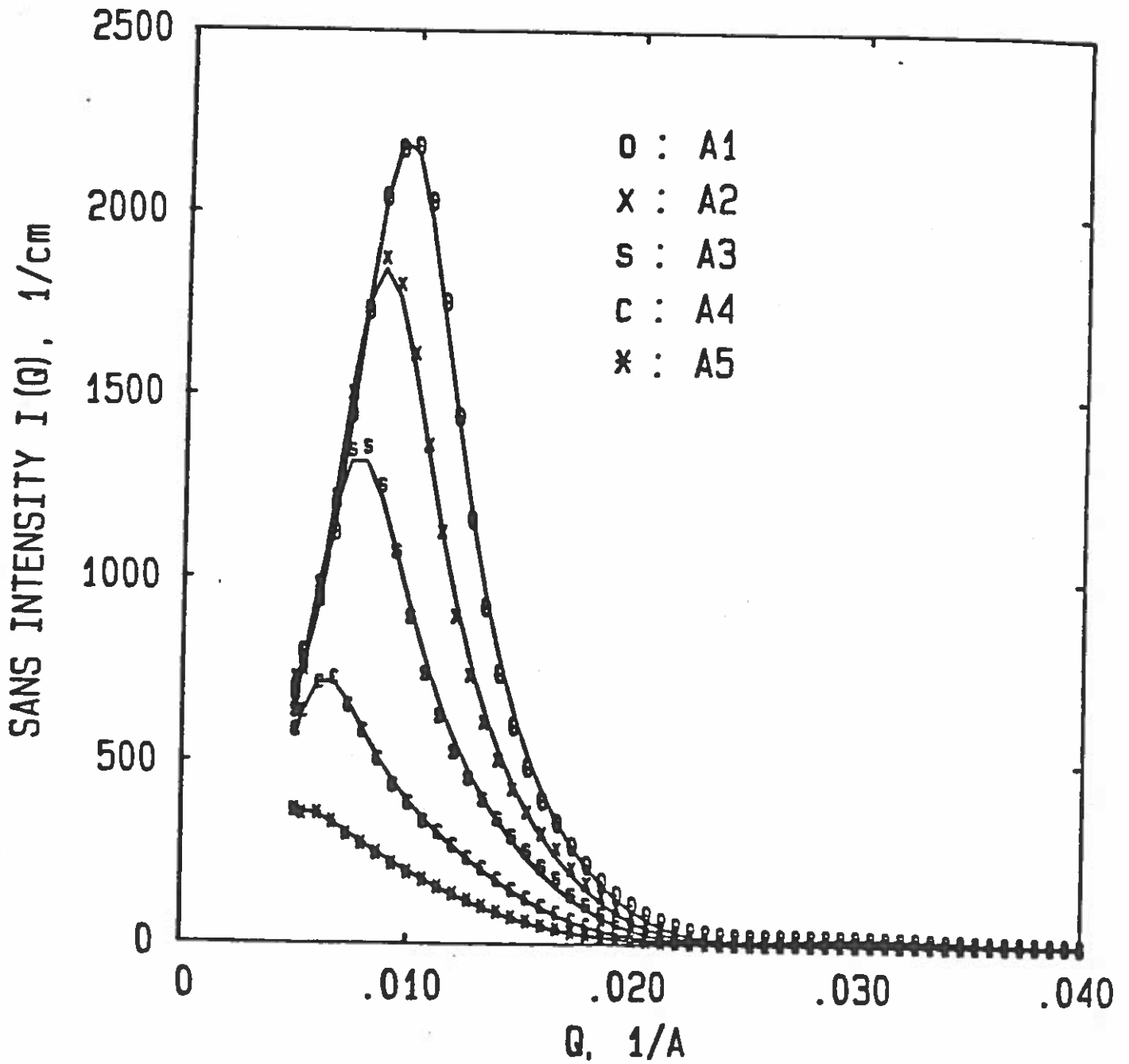
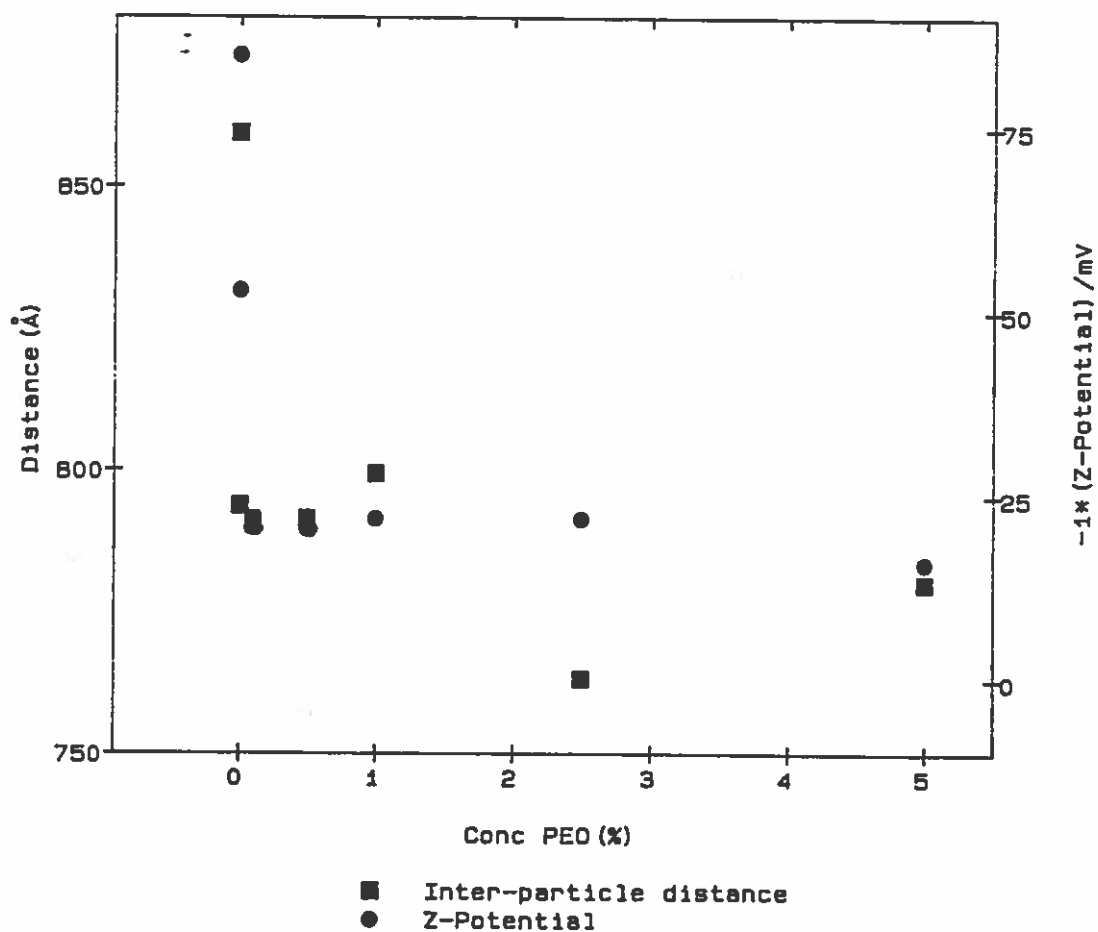


Fig. 1 Experimental (dots) and GOCM Fitted (solid curves) SANS Intensity profiles of polystyrene latex particles in deuterated water (88% D₂O (v/v))(Series A). The Polydispersity Width Parameter of this series is 100. The particle volume fractions of the samples A1, A2, A3, A4, and A5 are 0.0741, 0.0556, 0.0371, 0.0185, and 0.0095, respectively.

Fig. 2 Variation of inter-particle distance and zeta-potential of latex particles with the PEO (Mw=19.6K) concentration



CONC(%) OF PEO(19.6K)	INTER-PARTICLE DISTANCE(A)	Z-POTENTIAL (mV)
0.0	860	85
0.005	794	53
0.10	791	22
0.5	792	22
1.0	799	22
2.5	763	22
5.0	780	16

Contribution for the Department of Physical and Colloid Chemistry, Wageningen Agricultural University, P.O. Box 8038, 6700 EK Wageningen, The Netherlands.

EFFECT OF ADSORPTION ENERGY ON POLYMER LAYER THICKNESS

G.P. van der Beek, M.A. Cohen Stuart and J. Lyklema

What happens with the structure of adsorbed polymer layers when the binding strength between polymer segments and adsorbent is changed? One way to obtain information about this structure is to measure the hydrodynamic thickness of these adsorbed layers. Theoretical calculations have shown that this thickness is completely determined by the dilute periphery of the adsorbed layer. This region is dominated by dangling chain ends (tails). According to the Scheutjens-Fleer theory, the density profile of tails is almost independent of the segment adsorption energy parameter χ_s in contrast to the density of "loops", which varies strongly with this parameter. This means that the layer thickness should remain constant with decreasing χ_s , down to a value χ_{sc} , where complete desorption takes place. The transition between these two states is extremely sharp, much sharper than the corresponding change in adsorbed amount.

This theoretical result has been investigated by adsorption experiments of poly(ethylene oxide) PEO on small silica particles (ludox, $\phi = 30$ nm) in aqueous solutions. In this case, the segment adsorption energy can be reduced by increasing pH. The hydrodynamic layer thickness δ_h has been determined by Dynamic Light Scattering, which measures the diffusion coefficient of the particles. The adsorbed amount has been determined analytically, measuring the free polymer concentration colorimetrically. Fig. 1 presents both the adsorbed amount A and the layer thickness δ_h as a function of pH (χ_s). The curves agree very satisfactorily with the theoretical predictions.

The independence of δ_h of the adsorption energy suggests that for a given polymer in a given solvent δ_h should be the same for other substrates. This presumption is supported by data from Kawaguchi et al. (*Macromolecules*, 17, 2063 (1984)). They have determined δ_h of PEO on cellulose esters by a flow rate technique. Killmann et al. (*Colloids and Surfaces*, 15, 261 (1985)) have measured δ_h of PEO on larger silica particles ($\phi = 100$ nm) than investigated by us. Fig. 2 shows the agreement between δ_h of PEO on silica and cellulose esters in aqueous solutions for several molecular weights.

Unexpectedly, hydrodynamic PEO layers on polystyrene latex appear to be significantly thicker than those on other substrates (see also fig. 2). We suggest that this difference is due to the distribution of adsorption sites (distances between these sites). This idea is corroborated by an observation by Cosgrove (Polymer Comm., 28, 64 (1987)), who has found that PEO adsorption on latex depends on a few active surface sites.

This indicates that it is possible to obtain information about the PS surface by measuring the adsorbed PEO layer thickness. Further research is clearly needed to be more conclusive.

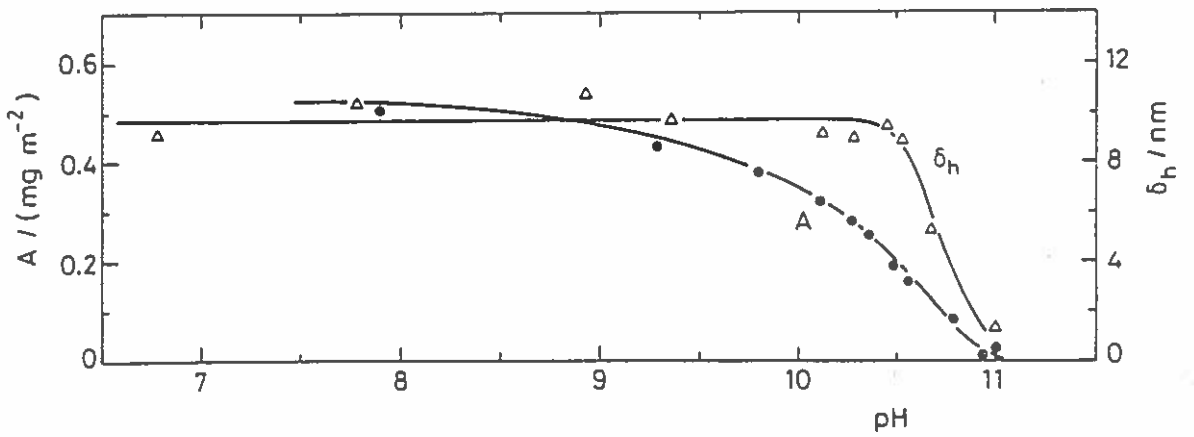


fig. 1 : Hydrodynamic layer thickness δ_h and adsorbed amount A as a function of pH for PEO ($M_w = 5,7 \cdot 10^5$) adsorbed on colloidal silica.

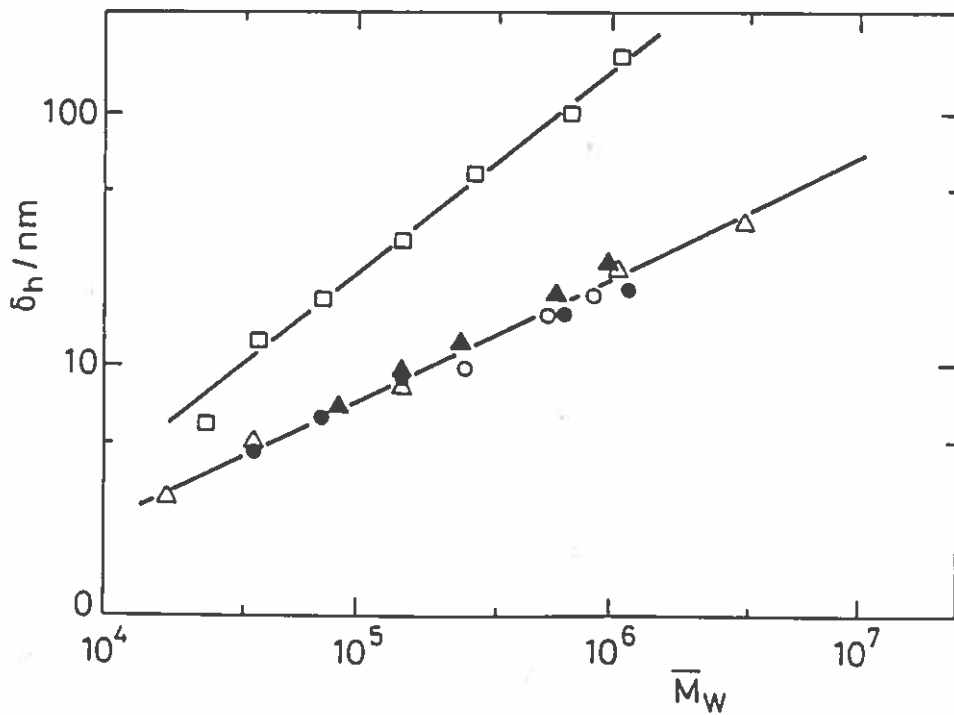


fig. 2 : Double logarithmic plot of δ_h (at saturation) as a function of molecular weight for PEO/water

- PEO on silica $\phi = 30$ nm (this work)
- △,▲ PEO on silica $\phi = 100$ nm (Killman et al.)
- PEO on cellulose esters (Kawaguchi et al.)
- PEO on PS latex (Cosgrove, *Macromolecules*, 17, 1825 (1984)).



POLYMER COLLOIDS AT THE UNIVERSITY OF SYDNEY

Reporter: D. H. Napper

More on Termination Events in Emulsion Polymerization

In the last Newsletter, we pointed out that termination events in the emulsion polymerization of methyl methacrylate appeared to be governed primarily by residual termination (i.e. termination arising from propagation) for which simple theoretical upper and lower bounds could be derived using Smoluchowski theory. We also noted that the situation with styrene as the monomer was more complex.

Mary Adams (formerly in our Group but now at Lehigh) has shown experimentally that residual termination is probably not the major termination mechanism in styrene emulsion polymerization systems, at least at lower right fractions of polymer. The experimental evidence for this is quite direct: relaxation measurements on γ -irradiated seeded emulsion polymerization's display at least two characteristic relaxation times. The faster relaxation process appears to be an order of magnitude too fast for it to be residual termination. It can however be interpreted as arising from termination events between free radicals attached to long, entangled polymer chains and free radicals attached to short, unentangled chains (so called 'short-long' termination). The latter are capable of centre-of-mass diffusion and move in this way to the free radicals attached to entangled chains, so that termination can occur. Note that as the fraction of short chains is relatively small (due to their rapid growth to greater than the entanglement length), short-short termination is relatively important. Long-long residual termination is also relatively unimportant, primarily because of its much lower rate coefficient.

It is possible to model the microscopic kinetic processes detailed above and from chemically and γ -initiated seeded kinetics, as well as relaxation data, to determine the rate coefficient for short-long (and thus short-short) and long-long termination events. The figure given below presents data for these two rate coefficients for styrene at 50°C as a function of the weight fraction of polymer present in the latex particle. Notice that the experimental values of k_p are several orders of magnitude smaller than the values of k_p listed in Polymer Handbooks for zero weight fractions of polymer.

Diffusion Controlled Propagation Rate Coefficients

Have you ever wondered what to do with that part of your kinetic data at high conversions where the rate of polymerization decays quite rapidly? There seems to have been very few attempts in the literature to interpret this this conversion data. Qualitatively, at least, the reason for the drop-off

is straightforward: the decline in rate arises from propagation becoming diffusion-controlled (it being assumed that the half-life of the initiator is sufficiently long not to intrude). In these circumstances, the decay in the polymerization rate reflects the decrease in k_p , the actual magnitude of k_p can be calculated if the value of the termination rate coefficient is known or can be predicted theoretically. It seems reasonable to assume that under conditions where k_p is diffusion controlled, k_p is controlled by residual termination in the rigid limit (see last Newsletter). Values of k_p for methyl methacrylate in the diffusion controlled domain at high conversions have been calculated using this method and compared with the values of k_p determined under the same conditions by ESR spectroscopy. The agreement between the two different methods is good.

Publications

1. D. H. Napper and R. G. Gilbert, Makromol. Chem. Makromol. Symp., 10, 503 (1987).
'Microscopic Kinetic Events in Emulsion Polymerization'
2. P. J. Feeney, D. H. Napper and R. G. Gilbert, J. Colloid Interface Sci. 118, 493 (1987).
'The Determinants of Latex Monodispersity in Emulsion Polymerizations'
3. P. J. Feeney, D. H. Napper and R. G. Gilbert, Macromolecules 20, 2922 (1987)
'Surfactant-free Emulsion Polymerizations: Predictions of the Coagulative Nucleation Theory'
4. G. A. Leslie, I. A. Maxwell, M. J. Ballard, R. G. Gilbert and D. H. Napper, Aust. J. Chem. 41, 279 (1988).
'A New Method for Determining Propagation Rate Coefficients at High Fractions of Polymer'
5. P. J. Feeney, E. Geissler, R. G. Gilbert and D. H. Napper, J. Colloid Interface Sci. 121, 508 (1988).
'SANS Study of Particle Nucleation in Emulsion Polymerization'

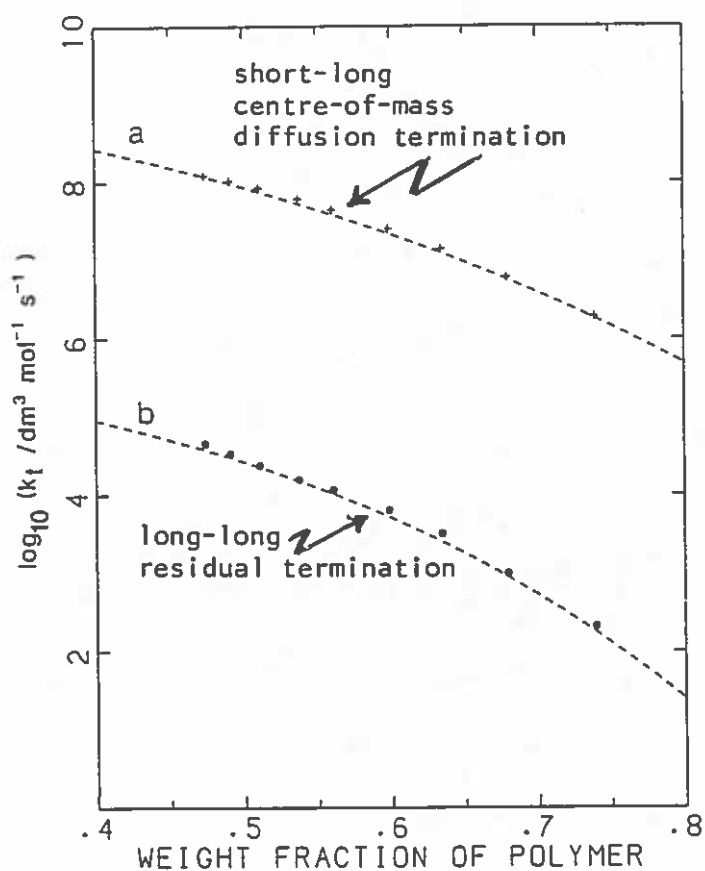


Figure 7.6 (+) $\log_{10}(k_{t1}/\text{dm}^3 \text{mol}^{-1} \text{s}^{-1})$ versus w_p and (x) $\log_{10}(k_{t2}/\text{dm}^3 \text{mol}^{-1} \text{s}^{-1})$ versus w_p determined from model fitting of experimental relaxation data. (a) Equation 7.7, (b) Equation 7.8.

Rapid Communications

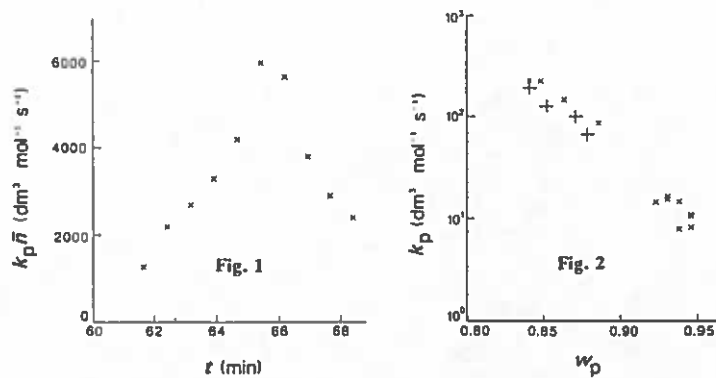


Fig. 1. Experimental rate data [as $q = V_S N_A d \ln(1-x)/dt$] for seeded emulsion polymerization of methyl methacrylate at 50°C. Unswollen particle radius is 68 nm; initiation by γ radiolysis, with multiple insertions into, and removals from, radiation source (data shown are for last insertion only). Experimental conditions otherwise are as for runs RG5-13 in ref. 5.

Fig. 2. Propagation rate coefficient k_p as function of w_p for methyl methacrylate: x deduced from c.s.r. data,¹ + deduced from data of Fig. 1 by the technique presented in this paper.

Contribution to Polymer Colloid Newsletter

R. Pelton and A. Hamielec

McMaster Institute of Polymer Production Technology

Particle sizes and electrophoretic mobilities of polyNIPAM latex.

R.H. Pelton, H.M. Pelton, A. Morphesis, and R. Rowell

Average particle diameters and electrophoretic mobilities of poly(N-isopropylacrylamide) latex were measured as a function of temperature. Diameters decreased from 788 nm at 10 °C to 380 nm at 50 °C in 0.001 M KCl; the corresponding electrophoretic mobilities increased from $-0.193 \times 10^{-8} \text{ m}^2\text{V}^{-1}\text{s}^{-1}$ (18 °C) to $-3.06 \times 10^{-8} \text{ m}^2\text{V}^{-1}\text{s}^{-1}$ (47 °C). The most dramatic changes with temperature occurred around 31 °C, the lower critical solution temperature of poly(N-isopropylacrylamide) in water. The increased electrophoretic mobility with temperature reflected increasing charge density when the particle diameter decreased. Charge density increased with decreasing particle diameter because the number of charged groups per particle was constant.

CONTRIBUTION TO POLYMER GROUP NEWSLETTER FROM LMO /CNRS(BP24
VERNAISON 69390-FRANCE) SUBMITTED BY C.PICHOT

1) MECHANICAL PROPERTIES OF LATEX FILMS OBTAINED BY EMULSION COPOLYMERIZATION OF STYRENE AND n-BUTYL ACRYLATE (B.SCHLUND,A.CRUIZ,C.PICHOT,J.GUILLOT)

Latexes with various particle morphologies have been prepared by different processes: batch, semi-continuous, multi-stage polymerizations or homopolymer blends. Films casted from these latexes were studied by mechanical spectroscopy in dynamic mode. Based on Kerner and Dickie approaches, a theoretical simulation of the mechanical properties was developed which gives a rather good account of the morphology of the films induced by the particle structuration.

2) COMPUTER SIMULATION OF THE GLASS TRANSITION TEMPERATURE (T_g) OF RANDOM COPOLYMER BLENDS (J.GUILLOT,W.RAMIREZ,S.DJEKHABA)

Batch emulsion copolymers of styrene with methyl or ethyl acrylate are found to be a complex mixture of macromolecules due to the large compositional drift induced by discrepancies in reactivity ratios and water solubilities of acrylate monomers. Assuming that each macromolecule keeps its own characteristic in the glass temperature phenomenon, a simulation permits to compute a theoretical DSC curve which takes into account the microstructure (dyads distribution), the T_g of both homopolymers and that of an ideally alternating copolymer as well their heat capacities. Comparison with experimental DCS data provides useful information on film formation and latex morphology.

3) COAGULATION STUDIES OF LOW SIZE COLLOID POLYSTYRENE BY HYDROSOLUBLE POLYMERS (M.JANER,C.GRAILLAT,C.PICHOT,A.REVILLON,A.GUYOT)

This work is currently investigated within a cooperative research program sponsored by the CNRS so as to understand the flocculation mechanisms of organic and mineral particles as well as the formation and structure of flocs in the presence high Mw polymers. The contribution of the lab in this program is to study the flocculation of well-characterized low size colloid PS (in the range of 40-50 nm) prepared in the presence of a sulfobetaine-type emulsifier. Different hydrosoluble polymers have been selected (polyacrylamides with various amount of a cationic comonomer, polyethylenoxides) so as to examine the effect of the nature and molecular weight on the flocculation mechanism. A turbidimetric method and the hydrodynamic chromatography technique are currently performed for studying the flocculation kinetics and the formation of flocs.

4) RECENT PUBLICATIONS.

-REACTIVITY RATIOS AND AZEOTROPY IN EMULSION COPOLYMERIZATION J.GUILLOT, *New Journal of Chemistry*, 11, n° 11/12, 787 (1987)

-COPOLYMERISATION EN EMULSION ACRYLATE D'ETHYLE-STYRENE. ETUDE CINETIQUE EN REACTEUR FERME, C.GRAILLAT, S.DJEKHABA, J.GUILLOT, *Eur. polym. J.*, 24, n° 2, 109 (1988)

-ETUDE CINETIQUE DE LA POLYMERISATION EN EMULSION DU STYRENE EN EMULSION EN PRESENCE D'EMULSIFIANTS AMPHIIONIQUES DE TYPE SULFOBETAINE
H.ESSADDAM, C.PICHOT, A.GUYOT, *Makromol. chemie* 189, 619 (1988)

-NARROW SIZE DISTRIBUTION POLYSTYRENE LATEXES PREPARED IN THE PRESENCE OF AMPHOTERIC SULFOBETAINE SURFACTANTS
H.ESSADDAM, C.PICHOT, A.GUYOT, *Colloid Polym J.*, 266, 1, (1988)

5) THE SECOND INTERNATIONAL CONFERENCE ON "Copolymerization and Copolymers in dispersed media" will be held in Lyon from 3-7 april 1989. See enclosed the first circular for detailed informations.

Newsletter contribution from the University of Akron,
Professor Inja Piirma;

Richard Flecksteiner, graduate student;

We are currently studying the emulsion polymerization of styrene using a mixture of the nonionic surfactant tridecyloxy poly(ethylene oxide) with 15 moles of ethylene oxide, commercially known as Emulphogene BC-840, and the cationic surfactant hexadecyltrimethylammonium bromide, abbreviated as HDTAB, as the surfactant. The molar percentage of the HDTAB is varied from 0 to 10% of the total surfactant mixture. The surfactant mixture is used at either 5 or 10 wt.% based on the monomer. The initiator is 2,2'-azobis(2-amidinopropane) hydrochloride and the temperature of the reaction is either 35 or 50 C.

We have found that at 35 C the rate of polymerization increased by 25% when the amount of HDTAB was increased from 2.5 to 5.0 mole% at a surfactant concentration of 5 wt.% based on monomer. At a surfactant concentration of 10 wt.% the rate of polymerization increased 36% for the same change in the surfactant composition. An increase of the HDTAB from 5 to 10 mole% of the surfactant had little effect on the rate of polymerization.

At 50 C we have found that using Emulphogene BC-840 alone as the surfactant resulted in two constant rate regions and a bimodal particle size distribution which are indicative of phase inversion occurring during the reaction. The addition of 2.5 mole% of HDTAB to the Emulphogene BC-840 causes the difference between the two constant rate regions to appear less pronounced. Increasing the amount of HDTAB to 5 mole% eliminated the two constant rate regions. The rate of polymerization increased by 30% when the HDTAB concentration was increased from 5 to 10 mole% of the total surfactant. The rate of polymerization was found to double when the surfactant concentration was raised from 5 to 10 wt% based on the monomer for every surfactant mixture used. Stable latices were unable to be produced using HDTAB as the only surfactant.

Research Progress by Wen-Lin Wu

Title: Synthesis of Polymeric Surfactants

An amphipathic polymeric surfactant was synthesized to be used in emulsion polymerization as a stabilizer. This surfactant consisted of poly(ethylene oxide) (PEO) as the stabilizing moiety and a polyamide (PA) as the anchoring moiety. The triblock of PEO-PA-PEO was prepared as follows:

Step A: An amorphous PA center block was synthesized by reacting excess 2,2,4-trimethylhexamethylenediamine with dimethyl terephthalate in water at 95°C for 10 hrs, followed by distilling off water and methanol under vacuum. Melt polycondensation was then carried out at 270°C for 3 hrs in vacuo to give an amine-terminated PA.

- Step B: The same-terminated PA was reacted with excess bromoacetyl chloride in DMF at room temperature for 4hrs in the presence of triethylamine to give a bromide-terminated PA.
- Step C: Poly(ethylene glycol methyl ether) (M_n = 5000) was treated with either sodium, sodium hydride, or potassium t-butoxide in DMF at 80°C for 8 hrs to form sodium or potassium alkoxides. The bromide-terminated PA from Step B in DMF solution was then added to the above solution over a period of 24 hrs to give a PEO-PA-PEO triblock copolymer.

Unfortunately a very low yield of the PEO-PA-PEO copolymer was obtained. The structure of the block copolymer was verified by both FTIR and NMR spectra. The low yield was probably due to the low reactivity of the bromide-terminated PA towards the Williamson synthesis with sodium or potassium alkoxides.

From: Gary Jialanella
Subject: Research Progress Report

Research work consists of synthesizing poly(ethylene oxide-g-methyl methacrylate) for use as a polymeric stabilizer in emulsion polymerization. Several methods which can be used to synthesize this copolymer have been examined; 1) polymerization of monomethoxy-poly(ethylene oxide) methacrylate with methyl methacrylate ii) ring opening of the epoxy group contained in a methyl methacrylate - glycidyl methacrylate copolymer by potassium terminated poly(ethylene oxide)-PEO iii) transesterification of poly(methyl methacrylate) with PEO. Although, all of these methods yield graft copolymers, the transesterification reaction seems to be the simplest method in which graft copolymers are obtained in high yield with a minimum amount of side reactions. However, published work consists of a two-step process in which potassium terminated PEO is prepared first, followed by the transesterification of poly(methyl methacrylate) in toluene. (J. Polym. Sci. A7, 2469 (1969)). By running the reaction in pyridine, a one-step process can be used, and the methanol by-product can be removed easily since methanol does not azeotrope with pyridine, thus improving the yield.

This graft copolymer was used as an amphipathic polymeric stabilizer for the emulsion polymerization of methyl methacrylate. Highly stable latices were prepared with an average particle size of 300 nm.

FREE RADICAL TRANSPORT FROM LATEX PARTICLES

R. N. Mead & G. W. Poehlein
Georgia Institute of Technology
Atlanta, GA 30332-0100

The transport of free radicals to and from the monomer-swollen latex particles is an important phenomenon in emulsion polymerization reactions. The early recursion equation of Smith and Ewart (1) for the number of particles containing 'n' free radicals includes terms for absorption and desorption of free radicals as well as for radical termination within the particles.

Polymerizing radical oligomers of any significant molecular weight are not expected to diffuse from the particles to the aqueous phase. Such molecules would normally be strongly hydrophobic and perhaps entangled with polymer molecules in the particles. Radical desorption is generally believed, therefore, to follow a transfer reaction in which a small, mobile free radical is formed. Such a radical could reinitiate polymerization by reacting with monomer or diffuse to the surface of the particle and cross the interface into the aqueous phase. Mathematical modeling of this phenomenon involves the classic concepts of diffusion with simultaneous chemical reaction.

Reactions and Mass Transfer Fundamentals

The chemical reactions that take place in an emulsion polymerization system which could influence radical desorption include chain transfer, reinitiation of polymerization, and termination. These reactions and related rate expressions are summarized below.

<u>Reaction</u>	<u>Mechanism</u>	<u>Rate</u>
Transfer to Monomer	$P^* + M \rightarrow P-H + M_m^*$	$k_{fm}[P^*]_p[M]_p$
Transfer to CTA	$P^* + T \rightarrow P-X + T^*$	$k_{TT}[P^*]_p[T]_p$
Reinitiation	$M_m^* + M \rightarrow P^*$	$k_p'[M_m^*]_p[M]_p$
	$T^* + M \rightarrow P^*$	$k_T'[T^*]_p[M]_p$
Termination	$P^* + P^* \rightarrow \text{Dead Poly}$	$k_t[P^*]_p^2$
Propagation	$P^* + M \rightarrow P^*$	$k_p[P^*]_p[M]_p$

The long-chain free radical is P^* and M_m^* is the monomer free radical. The rate constants for chain transfer to monomer and chain transfer agent, T, are k_{fm} and k_{TT} , respectively. The

rate constants for reinitiation of oligomer radicals from M_m^* and T^* radicals are k_p' and k_T' , respectively. The net rate of monomer radical formation, R_A , is the rate of chain transfer to monomer minus the rate of reinitiation of oligomer radicals by monomer radical propagation.

$$R_A = k_{fm}[P^*]_p[M]_p - k_p'[M_m^*]_p[M]_p \quad (1)$$

Ugelstad and Hansen (2) observed that k_p' may not be equal to the rate constant for the propagation of oligomer radicals, k_p .

The process of monomer free radical transport from latex particles can result in concentration gradients within the particle and in the aqueous phase as shown in Figure 1. For this example $[P^*]_p$ is assumed to be constant with respect to radial position in the particle. C_p is the position-dependent concentration of monomer free radicals within the particle. The monomer free radical concentration at the particle side of the particle-water interface is C_{ps} and the concentration at the water side of the interface is C_{ws} . Ugelstad and Hansen (2) assumed C_{ws} was related linearly to C_{ps} as in Equation 3.

$$C_{ws} = C_{ps}/a \quad (2)$$

The term "a" is the partition coefficient for monomer free radicals between the aqueous and particle phases.

Models for concentration profiles and transport rates in non-convective systems are obtained by shell balances. Equation 3 is the fundamental steady-state differential equation for transport with chemical reaction of any species in a symmetrical spherical system.

$$\frac{d}{dr}(r^2N) = r^2R_A \quad (3)$$

The radial distance from the center of the sphere is r , N is the diffusive flux in moles per unit of time normal to the radial direction and R_A is the net rate of reaction of the diffusing species in moles per unit volume-time. In the absence of bulk flow of the diffusing species the flux is given by Fick's first law.

Ugelstad and coworkers (2,3,4) and Nomura et al. (5,6,7) derived Equation 4 for Q_w , the mass transfer rate on the water side of the particle-aqueous phase interface.

$$Q_w = 4\pi RD_w(C_{ws}-C_{wi}) \quad (4)$$

The following boundary conditions were used:

$$r = R \quad C_w = C_{ws} \quad i$$

$$r \rightarrow \infty \quad C_w = C_{wi} = 0 \quad ii$$

Ugelstad and Hansen (2) assumed that chain transfer and reinitiation reactions are negligible in the aqueous phase, thus $R_A = 0$ when Equation 3 is applied to the diffusion of radicals in the aqueous phase.

The derivation of an expression for the mass transfer rate on the particle side of the interface, Q_p , is more difficult because monomer free radicals will be produced by chain transfer and consumed by reinitiation within the particle. Ugelstad and Hansen (2) presented an expression for Q_p which is given by Equation 7.

$$Q_p = -4\pi R D_p (C_{ps} - C_p^*) \quad (5)$$

The diffusivity of monomer radicals in the particle is D_p . C_p^* was defined as "the mean radical concentration in the middle of the particle." Ugelstad and Hansen stated that "this is the same as the mean concentration of radicals in the particle, because the radical is formed at a random point in the particle and has a mean diffusion path $L=R$."

The appropriate boundary conditions, however, for steady-state monomer free radical transport from latex particle are presented below.

$$\text{at } r = 0 \quad dC_p/dr = 0 \quad iii$$

$$\text{at } r = R \quad C_p = C_{ps} \quad iv$$

If boundary conditions iii and iv are used with Equation 3 when R_A is nonzero, the expression obtained for Q_p is not the same as that derived by Ugelstad and Hansen (2).

The derivation of Ugelstad and Hansen's expression for Q_p is unclear, however, if Equation 5 is accepted as a valid expression for Q_p , the derivation of the desorption rate constant can be completed by equating Q_p and Q_w and using Equation 2 to obtain the following relation for C_{ws} .

$$C_{ws} = \frac{C_p^*}{a + (D_w/D_p)} \quad (6)$$

The steady-state mass transfer rate of monomer free radicals from the particle is Q .

$$Q = \frac{4\pi R <C_p> D_w}{(a + D_w/D_p)} \quad (7)$$

The mean concentration of monomer free radicals is the particle, $\langle C_p \rangle$, is equal to $n_m/v_p N_A$. The average number of monomer radicals per particle is n_m and v_p is the volume of the monomer-swollen particle. The monomer free radical desorption constant, k_{dm} , is given by Equation 8 in units of s^{-1} .

$$k_{dm} = \frac{Q}{\langle C_p \rangle v_p} = \frac{12D_w}{(a + D_w/D_p)d_p^2} \quad (8)$$

The diameter of the monomer-swollen particle is d_p . The desorption coefficient used in emulsion polymerization models is normally applied to the average of the total number of radicals per particle. Ugelstad and Hansen (2) derived an expression for k_d as in Equation 9.

$$k_d = \frac{k_{fm}}{k_p} k_{dm} \quad (9)$$

Ugelstad and Hansen (2) obtained an expression for k_d by combining Equations 8 and 9.

$$k_d = \frac{k_{fm}}{k_p} \left\{ \frac{12D_w}{(a + D_w/D_p)d_p^2} \right\} \quad (10)$$

The particle-size-independent desorption rate constant is k_d' .

$$k_d' = k_d v_p^{2/3} = \frac{k_m}{k_p} \left\{ \frac{12(\pi/6)^{2/3} D_w}{a + D_w/D_p} \right\} \quad (11)$$

Nomura et al. (5,6,7) derived a similar expression for k_d' independently of Ugelstad et al. (2).

Extension of Monomer Radical Transport Theory

Neither Ugelstad et al. or Nomura et al. considered the case where the monomer free radical concentration could vary significantly within the particle. This could occur for two reasons: (1) very low diffusivity of monomer free radicals in the particle or (2) a nonuniform generation of free radicals within the particle. These phenomena are considered separately in the following two sections.

Diffusion-Limited Transport Form Particles

If the oligomer free radicals and monomer molecules are assumed to be distributed uniformly in the particle, the monomer free radicals will be produced at a constant rate everywhere within the particle. The monomer free radical concentration, however, may not be constant with respect to radial position in the particle if the diffusivity of the monomer free radical is low.

The following section includes the results of a derivation of a desorption rate constant based on the assumption that oligomer free radicals are distributed uniformly in the particles. The derivation differs from the previous models because reinitiation of monomer radicals to form oligomer chains is coupled with diffusion considerations.

The assumptions used in the derivation are: (1) a steady-state monomer free radical concentration profile is established; (2) the oligomer free radicals are distributed uniformly throughout the particle; (3) monomer free radicals may reinitiate oligomer chains by adding a monomer molecule; and (4) the concentration of monomer free radicals at the particle surface is in equilibrium with the concentration of monomer free radicals on the water side of the particle-water interface as described by Equation 2. The monomer free radical concentration in the aqueous phase at infinite distance from the particles is assumed to be zero.

Chern (8) developed a steady-state balance on monomer free radicals about a differential element of the particle which yields the following equation.

$$D_p \frac{d^2 C_p}{dr^2} + \frac{2D_p}{r} \frac{dC_p}{dr} - k_p' [M]_p C_p = -k_{fm} [M]_p [P^*]_p \quad (12)$$

The following boundary conditions apply:

$$\begin{array}{ll} \text{at } r=0, & dC_p/dr=0 \\ \text{at } r=R, & v_i \end{array}$$

$$\frac{4\pi R D_w C_{ps}}{a} = \frac{4}{3}\pi R^3 (k_{fm} \langle [P^*]_p \rangle - k_p' \langle C_p \rangle) [M]_p$$

The volume-average concentration $\langle C_p \rangle$ is defined in Equation 13.

$$\langle C_p \rangle = \frac{4\pi \int_0^R C_p r^2 dr}{\frac{4}{3}\pi R^3} \quad (13)$$

Chern did not assume the oligomer radical concentration $[P^*]_p$ was uniform throughout the particle, so he could not obtain an analytical solution for Equation 13. In this work the oligomer free radicals are assumed to have a uniform distribution throughout the particle in order to obtain an analytical solution to Equation 12 which is given by:

$$C_p = \frac{k_{fm} [P^*]_p}{k_p'} \left[1 - \frac{2D_w \sinh(\phi r')}{\{ak_p' [M]_p R^2 X/3 + 2D_w \sinh(\phi)\} r'} \right] \quad (14)$$

$$\text{where: } \phi = R \left[\frac{k_p' [M]_p}{D_p} \right]^{1/2}$$

$$r' = r/R; X = 6 \left[\frac{\cosh(\phi)}{\phi} - \frac{\sinh(\phi)}{\phi^2} \right]$$

The volume-average concentration is given by:

$$C_p = \frac{k_{fm}[P^*]_p}{k_p'} \left[1 - \frac{D_w X}{\{ak_p'[M]_p X R^2/3 + 2D_w \sinh(\phi)\}} \right] \quad (15)$$

The oligomer radical concentration $[P^*]_p$ is given by:

$$[P^*]_p = \frac{\bar{n}}{N_A v_p} \left[1 - \frac{k_{fm}}{k_p'} \right] \quad (16)$$

Figure 2 is a plot of C_p versus dimensionless radius for ST emulsion polymerization at 60°C. The parameters used in the calculation are listed in Table 1. The value of \bar{n} used in the calculation of $[P^*]_p$ was 0.5; thus $[P^*]_p$ was assumed to be constant.

Table 1. Parameters for Styrene Emulsion Polymerization Simulation

Parameter		Source
T	60°C	-----
k_{fm}	8.8E-3 l/mole-s	Odian (13)
k_p'	176 l/mole-s	Lee (9)
D_w	2.0E-5 cm ² /s	Wilke and Chang (14)
a	1300	Lee (9)
D_p	Varied	

Lee (9) used the data of Goffloo (10) to estimate D_p as 2.0E-6 for ST-saturated polystyrene particles. The concentration profile for a D_p of 2.0E-6 is relatively constant while the profiles for D_p equal to 2.0E-8 and 2.0E-11 show an increased concentration in the bulk of the particle with a larger concentration gradient near the particle surface. The concentration profiles in Figure 2 indicate that the surface concentration C_{ps} , decreases with decreasing D_p . This phenomenon is consistent with the second boundary condition for Equation 12.

If $[P^*]_p$ is constant, $\langle C_p \rangle$ will increase when D_p decreases and the net rate of production of monomer free radicals (RHS b.c. vi) will decrease. The decrease in net production is balanced by a reduction in C_{ps} and Q . The decreasing values of C_{ps} with decreasing D_p are also consistent with Ugelstad and Hansen's theory. The flux at the surface, Q , defined by Equation 5, must be equal to the flux defined by Equation 7. These criteria have been verified numerically for the ST emulsion polymerization example.

Desorption Rate Constant

The flux of monomer free radicals at the particle surface, Q_p , is given by:

$$Q_p = 4\pi R^2 D_p \left. \frac{dc_p}{dr} \right|_{r=R} \quad (17)$$

The monomer free radical desorption constant, k_{dm} , is defined by:

$$k_{dm} = \frac{Q}{\langle C_p \rangle v_p} \quad (18)$$

The expression for k_d' is given by:

$$k_d' = k_d v_p = \left\{ \frac{k_{fm}}{k_p} \right\} k_{dm} v_p^{2/3} \quad (19)$$

Equation 17, the expression for $\langle C_p \rangle$ (Equation 15), the expression for k_{dm} (Equation 18), and the expression for k_d' (Equation 19) are combined to derive an expression for k_d' .

$$k_d' = \frac{k_{fm}}{k_p} \left[\frac{12(\pi/6)^{2/3} D_w}{a + \frac{D_w \{ \sinh(\phi) (1+3/\phi^2) - 3 \cosh(\phi)/\phi \}}{k_p' [M]_p R^2 [\cosh(\phi)/\phi - \sinh(\phi)/\phi^2]}} \right] \quad (20)$$

Ugelstad and Hansen's expression for k_d' differs in form from Equation 20 because of the assumption of uniform monomer free radical concentration. Equation 20 and Ugelstad and Hansen's equation for k_d' should give the same values for k_d' in the limiting case where D_p is relatively large and the concentration is uniform. This case corresponds to a small value of ϕ in Equation 20. Figure 3 is a plot of k_d' versus ϕ . The values of k_d' calculated using Ugelstad and Hansen's equation and Equation 20 both converge as ϕ approaches zero and D_p becomes relatively large. As D_p decreases Ugelstad and Hansen's equation for k_d' predicts a much smaller desorption constant than Equation 20. Ugelstad and Hansen's model cannot account for an increasing nonuniform distribution of monomer free radicals in the particle as D_p decreases.

Nonuniform Monomer Radial Generation

Chern (8) considered the case where the oligomer free radicals are nonuniformly distributed in the particle. Chern assumed the nonpropagating end of the growing polymer chain is anchored to the surface of the particle by the hydrophilic initiator end group and that the growing free radical end is free to propagate in any direction within the particle.

He developed an expression for $[P^*]_p$ as a function radical position in the particle.

$$[P^*]_p = \frac{1.43\bar{n}}{N_A v_p} \left(1 - \frac{k_{fm}}{k_p} \right) \exp \left\{ -k \left(1 - \frac{r}{R} \right) \right\} \quad (21)$$

The parameter k was determined from Monte Carlo simulations of the growth of a long-chain free radical in the latex particle. Chern calculated $[M_m^*]_p$ as a function of radial position by a simultaneous numerical solution of Equation 21 and the differential equation for diffusion and reaction of the monomer free

radical. Monomer free radical concentration profiles calculated by Chern for ST emulsion polymerization are presented in Figure 4. The parameters used in the calculation are included in Table 3. Chern's model predicts that the oligomer free radical is more likely to reside close to the particle surface, hence the rate of production and concentration of monomer free radicals are greater near the surface.

Chern used Equation 21 to develop an expression for k_d' which is shown below.

$$k_d' = \frac{k_{fm}}{k_p'} \frac{(4\pi/3)D_w}{a\{1/k' - 1/k'^2 = 2/k'^3\} - 2\exp[-k']/k'^3} \quad (22)$$

Chern used the parameters in Table 3 to calculate k_d' for ST emulsion polymerization with his model, Ugelstad's Equation 14, and Nomura's Equation 15. The results summarized in Table 3 indicate that Chern's model predicts a k_d' value similar in magnitude to the k_d' predicted by Ugelstad and Nomura's equations when D_p is relatively large. Chern's model predicts a much greater value of k_d' than the other models when D_p is relatively small. Chern's model predicts $[P^*]_p$ will be greatest near the surface, hence the monomer radicals have a shorter distance to diffuse before leaving the particle.

Table 2. Calculated Desorption Rate Constants for Styrene Emulsion Polymerization (Chern, 19878)

		k_d' (cm ² /s)	
D_p (cm ² /s)		Chern	Ugelstad, Nomura
$2.0 \cdot 10^{-6}$		$2.3 \cdot 10^{-13}$	$6.0 \cdot 10^{-13}$
$2.0 \cdot 10^{-9}$		$2.6 \cdot 10^{-13}$	$6.9 \cdot 10^{-14}$
$T = 60^\circ\text{C}$	$K_{fm} = 8.8 \cdot 10^{-3}$		1/mole-s
	$k_p' = 1760$ 1/moles-s		$D_w = 2.0 \cdot 10^{-5}$ cm ² /s
	$a = 1300$		

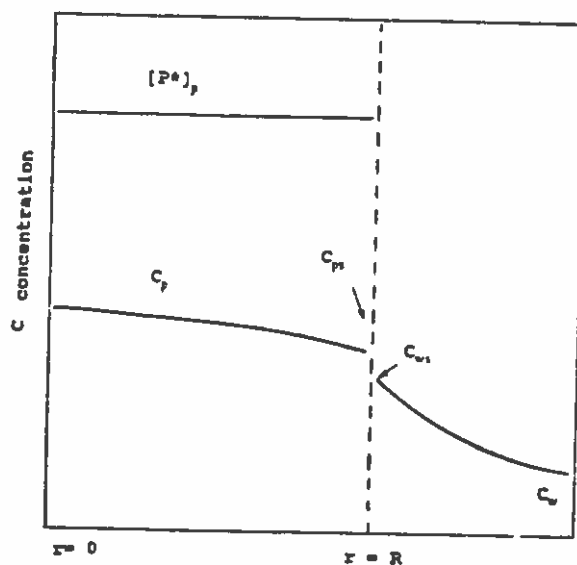


Figure 1. Concentration Profiles of Monomer Free Radicals

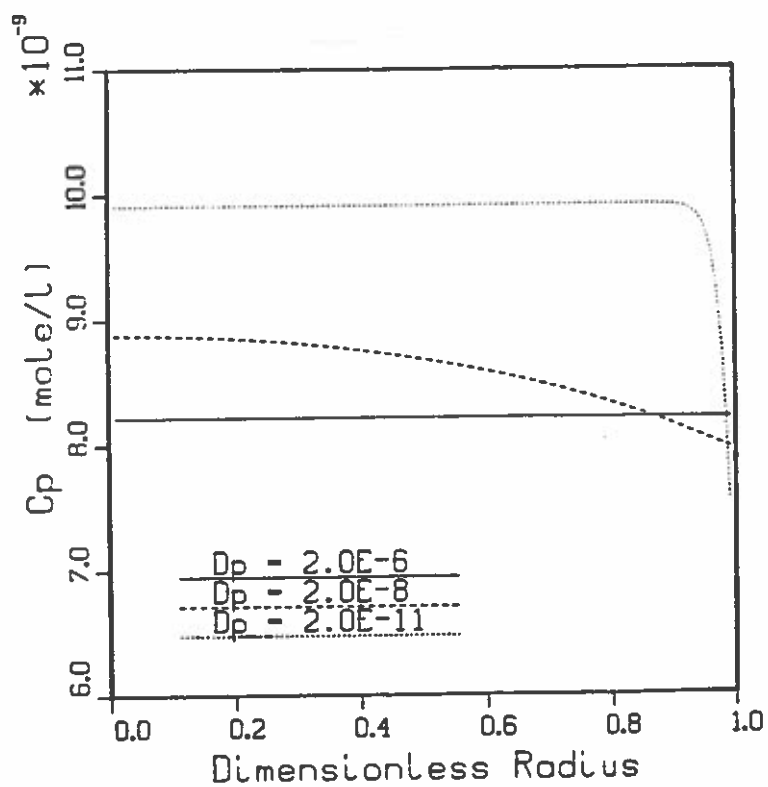


Figure 2. Calculated Monomer Radical Concentration Profiles for Styrene Emulsion Polymerization.

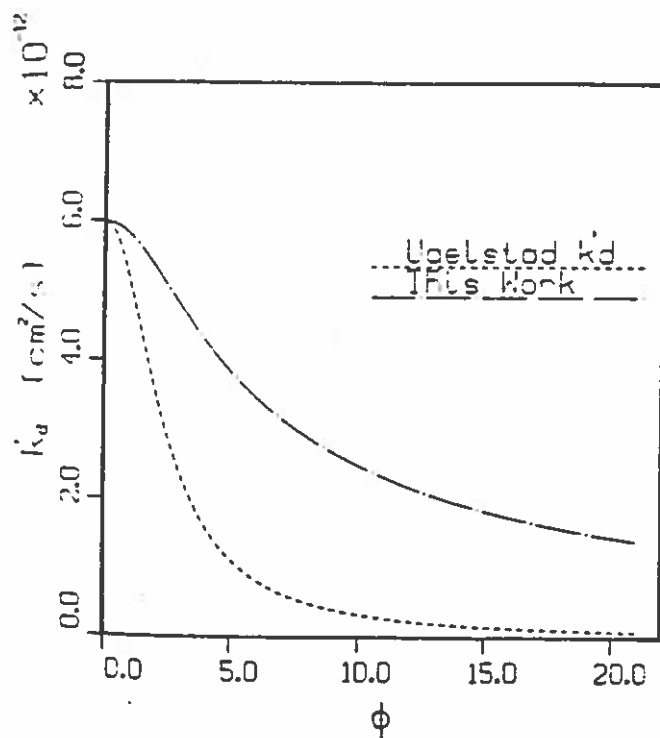


Figure 3. Calculated k_d' versus ϕ for Styrene Emulsion Polymerization.

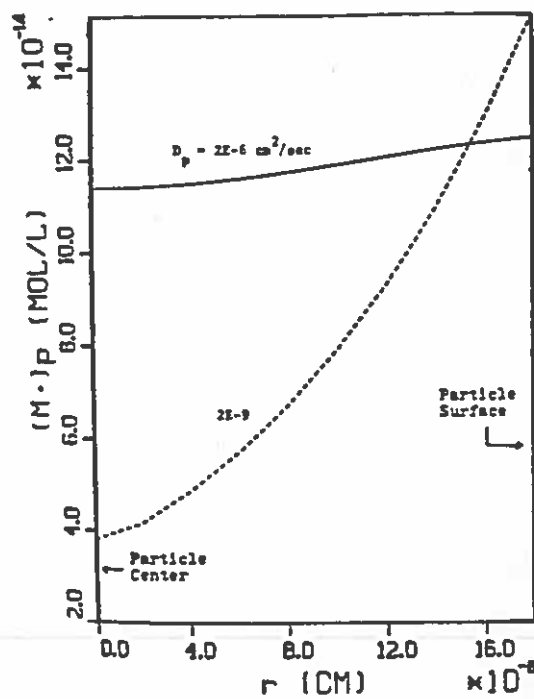


Figure 4. Monomer Free Radical Concentration Profiles. Chern (1987).

Bibliography

1. W. V. Smith and R. H. Ewart, J. Chem. Phys., 16, 592 (1948).
2. J. Ugelstad and F. K. Hansen, Rubber Chem. and Tech., 49, 536 (1976).
3. J. Ugelstad, P. C. Mork and J. O. Aasen, J. Polym. Sci., A-1, 5, 2281 (1967).
4. J. Ugelstad and P. C. Mork, British Polym. J., 2, 31 (1970).
5. M. Nomura, M. Harada, K. Nakagowara, W. Eguchi, and S. Nagata, J. Chem. Eng. Japan, 4, 160 (1970).
6. M. Nomura, M. Harada, W. Eguchi and S. Nagata, J. Apply. Polym. Sci., 15, 675 (1971).
7. M. Nomura, H. Kojima, M. Harada, W. Eguchi and S. Nagata, Paper 6 in "Emulsion Polymerization," I. Piirma and J. C. Gardon, Eds., ACS Symposium Series, 24, 102 (1976).
8. C. S. Chern, PhD Dissertation, School of Chemical Engineering, Georgia Institute of Technology, Atlanta, Georgia 30332 (1987).
9. H. C. Lee, PhD Dissertation, School of Chemical Engineering, Georgia Institute of Technology, Atlanta, Georgia 30332 (1985).
10. K. Goffloo and R. Kosfeld, Angew. Makromol. Chem., 37, 105 (1974).
11. M. Nomura, K. Yamamoto, I. Horie and K. Fujita, J. Apply. Polym. Sci., 27, 2483 (1982).
12. M. Nomura, M. Kubo and K. Fujita, J. APply. Polym. Sci., 28, 2767 (1983).
13. G. Odian, "Principles of Polymerization," Second Ed., John Wiley and Sons, New York (1981).
14. C. R. Wilke and P. Chang, AIChE J., 1(2), 264 (1955).

**POLYSAR LIMITED
POLYSAR LIMITÉE**

Sarnia Ontario Canada N7T 7M2

Telephone (519) 337 8251
Cable POLYSAR
Telex 064 76158**Contribution from Polysar Ltd. Latex Division for the Polymer Colloid
Newsletter**

Reported by Koichi Takamura

A paper describing colloidal characterization of styrene-butadiene latices has been presented at the 24th Canadian High Polymer Forum, August 5-7, 1987.

**MEASUREMENT AND APPLICATION OF COAGULATION RATE CONSTANTS IN COLLOIDAL
CHARACTERIZATION OF FUNCTIONALIZED STYRENE-BUTADIENE LATICES**

by K.P. Lok, C.A. Midgley, H.S.G. Slooten, J.J. Spitzer.

Functionalized styrene-butadiene latices (FSBL) have found important applications in papercoating, vinyl flooring, carpet-backing and adhesive industries, and they are now also being increasingly used in bitumen and concrete formulations. In all these applications the FSBL are compounded, often at high solids, with other materials, usually fillers, to give a colloiddally stable slurry that may be destabilized by water removal, or less often by addition of coagulating agents. In order to be able to design latices with predictable application performance, a program of colloid studies was initiated to characterize these latices.

This paper focuses on measurement of the initial coagulation rate constants for polymer particles manufactured by different recipes and processed in dilute aqueous solutions. Preliminary results of these measurements, together with electrophoretic mobility results, have been rationalized in terms of a qualitative "hairy particle" model, though other interpretations may also be possible.

The following two papers have been accepted in J. Colloid Interface Science for publication. The work was conducted during the time I was at the Alberta Research Council in Edmonton, Alberta.

ELECTROPHORETIC MOBILITIES OF BITUMEN AND CONVENTIONAL CRUDE-IN-WATER EMULSIONS USING THE LASER DOPPLER APPARATUS IN THE PRESENCE OF MULTIVALENT CATIONS.

ABSTRACT

A laser Doppler apparatus equipped with narrowly gapped platinized platinum electrodes was used to study the electric properties of bitumen-in-water and Moutray conventional crude-in-water emulsions over a wide range of NaCl concentrations and pH. It was found that a dilute buffer solution had to be used to prevent pH drift from occurring on the electrode surfaces. Analysis of the measured mobility using the Ionizable Surface-Group model revealed that the negative charges of both emulsions were due to the dissociation of carboxylic acids, though Moutray crude oil had only a quarter of the acid groups that existed on the bitumen surfaces.

Experiments were also conducted in the presence of Ca^{++} and Mg^{++} . The measured mobilities for both emulsions were again adequately explained by the model when the ion-binding of the cations with the acid groups was included. Several mobilities measured under the presence of the strong electrophoretic relaxation (10^{-4} M CaCl and CaCl_2) exceeded theoretical maximum values predicted by O'Brien and White's computer solution, thus suggesting that their theory might over estimate the relaxation effect.

EFFECTS OF SURFACE ROUGHNESS (HAIRINESS) OF LATEX PARTICLES ON THEIR ELECTROKINETIC POTENTIALS

ABSTRACT

In a previous paper, we demonstrated that the electric properties of the bitumen/water and crude oil/water interfaces could be explained by the dissociation of carboxyl groups belonging to natural surfactants present in bitumen. Electrophoresis of bitumen-in-water emulsions indicated vary high zeta potentials (-100 mV in 10^{-2} M NaCl) especially when compared to a carboxylated latex (-50 mV in 10^{-2} M NaCl) having similar surface charge density. This difference was attributed to the surface roughness of the latex particle, which results in a larger value for the location of the shear plane resulting in a smaller value for the zeta potential. To test this hypothesis we modified the surface roughness of the latex by heating it above its glass transition temperature. The heat treatment resulted in a significant increase of the zeta potentials calculated from the measured electrophoretic mobilities. This observation suggests that surface roughness (hairiness) is one of the most important factors in determining zeta potentials from electrophoresis. Results of electrophoretic mobilities of the original and heat treated latexes will be shown as a function of pH in a wide range of NaCl concentrations, and will be compared with those predicted by the Ionizable Surface-Group model. In addition, results of measured mobilities of the heat treated latex in NaCl, CaCl_2 , and $\text{La}(\text{NO}_3)_3$ below 10^{-4} M suggest that the computer solution of O'Brien and White over estimates the electrophoretic relaxation effect of $\chi a < 100$, where χ is the reciprocal Debye Huckel length, and a is the particle radius.

REPLY TO
RESEARCH LABORATORIES
727 NORRISTOWN ROAD
SPRING HOUSE, PA. 19477
(215) 641-7000
(215) CH 2-0400

The following abstract and selected figures are from a paper to be presented by Dr. R.G. Aviles at the 14th International Conference in Organic Coatings Science and Technology, Athens, July, 1988. Of special interest to the group would be the "lobed" acrylic latex particles and their viscosity characteristics. (Submitted via Pete Sperry)

ADVANCES IN RHEOLOGY CONTROL OF AQUEOUS COATINGS:
FROM ADDITIVES TO LATEX DESIGN

J.M. Rokowski, E.J. Schaller, and R.G. Aviles

Rohm and Haas Company
Research Laboratories, Spring House, PA 19477, USA

Recent advances in the technology of hydrophobically modified water soluble polymers have been applied to design new nonionic urethane associative thickeners possessing complementary viscosity/shear rate responses. Combinations of these thickeners can be used to control the rheology of aqueous coatings; without the need for additional surfactants and cosolvents. The fundamental rheological characteristics of the new thickeners are discussed in terms of their effect on paint rheology. In addition, novel acrylic latexes consisting of lobed particles, which provide increased viscosity over a broad range of shearing conditions, are also discussed. Theoretical predictions on the lobed particles contribution to volume fraction and viscosity, and on their interaction with associative thickeners, are presented and compared with experimental results.

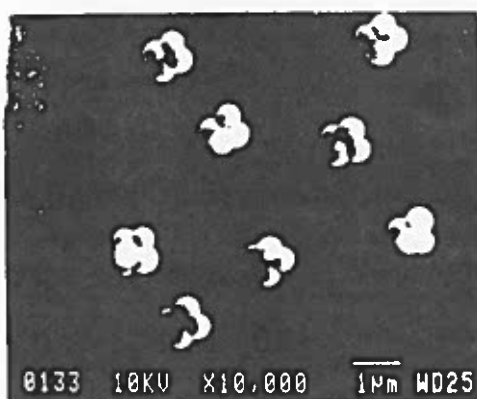
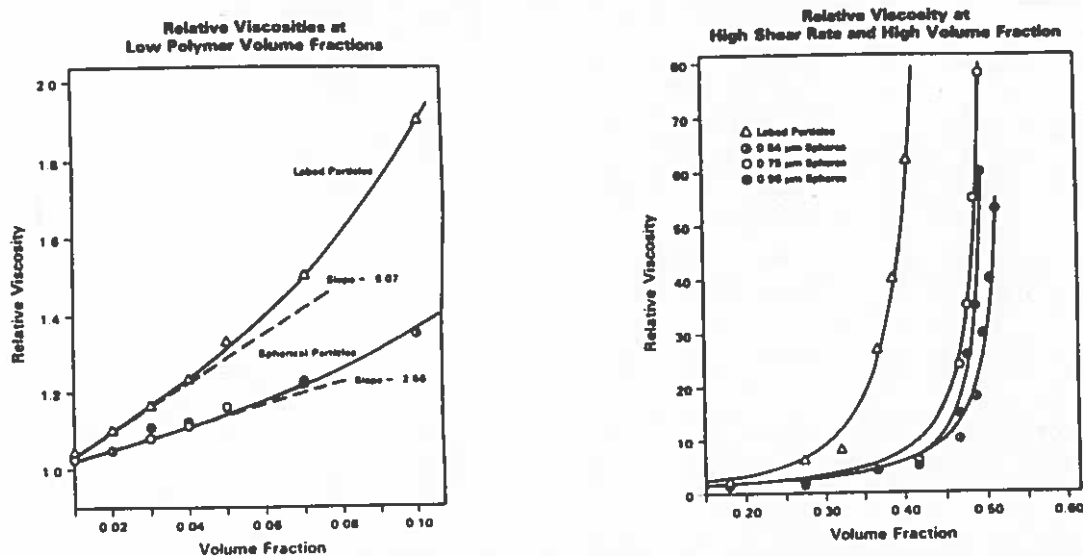


Figure 11. Scanning electron micrograph of lobed polymer dispersion.





UNIVERSITY OF MASSACHUSETTS AT AMHERST

Department of Chemistry

Lederle Graduate Research Center
Amherst, MA 01003

CONTRIBUTION FROM ROBERT L. ROWELL

Below are abstracts of papers presented at the Denver ACS meeting last fall. They are in press for publication in ENERGY and FUELS.

THE ELECTROPHORETIC MOBILITY DISTRIBUTION IN AQUEOUS DISPERSIONS OF BITUMINOUS COAL AND RESIDUAL HYDROCARBON MATERIALS

R.E. Marganski* and R.L. Rowell

Department of Chemistry
University of Massachusetts
Amherst, MA 01003

INTRODUCTION

The effect of mineral content on the electrokinetics of coal is very pronounced and contributes to a more hydrophilic surface that contains a substantial quantity of bound water. Mineral composition is known to vary markedly from coal to coal as does water content. Dewatering is an important aspect of coal preparation (1). In addition, there is evidence that the native mineral residue in coal plays an important catalytic role in direct hydro-liquefaction.

All of the above can be related to the electrophoretic behavior of the coal surface which in turn depends on the surface functional groups present. Even though intrinsic heterogeneity in coal produces no single and universal structure, enough similarity exists in these functionalities to predict the surface charging mechanisms. Previous explanation for surface charging on coal, based on oxide-like hydration and dissociation, fail to explain the positive charge at low pH so that the surface functionalities involved must include more than simple oxide groups.

These ideas were extended to the surface chemistry of residual hydrocarbon materials, the unconverted vacuum bottoms (uvb), obtained in petroleum refining. The uvb products are an unknown material that may have an asphaltene character, but the test is not conclusive. A significant result of this work was the finding that the electrophoretic properties of the uvb products resemble bituminous coal.

Coal fines and uvb products have not been commercially successful materials in the past. Recent efforts in coal-oil and coal-water systems, utilizing pulverized coal, have been promising. A similar role may be foreseen for the uvb products in slurry form.

In this paper, we report the full electrophoretic mobility distribution for several bituminous coals and a friable uvb sample as a function of pH in aqueous media. A discussion of the main structural features that effect electrophoresis is presented. The key parameters include determination of heteroatoms, carbon framework, mineral matter and physical structure, especially pores.

A COMPARISON OF THE ACOUSTIC MOBILITY AND THE ELECTROPHORETIC MOBILITY OF COAL DISPERSIONS

B.J. Marlow

Pen Kem, Inc.
Bedford Hills, NY 10507

R.L. Rowell

Department of Chemistry
University of Massachusetts
Amherst, MA 01003

INTRODUCTION

Aqueous coal dispersions play a major role from mining to the utilization of coal. The properties of these dispersions, such as stability towards aggregation, rheology, etc., are controlled by two major factors, namely, the particle size and interfacial chemistry. The interfacial chemistry is controlled by the interactions of the coal surface with the aqueous phase.

Coal surface-aqueous phase interactions are controlled by rank, mineral content, surface functional groups, pore structure, adsorption, pH, ionic strength, etc. These interactions can be probed using electrokinetic techniques (1-11). Electrokinetic techniques presently used to investigate aqueous coal dispersions include microelectrophoresis and streaming potential (12). Although both of these techniques are invaluable to study coal surface interactions they cannot be used for process condition dispersions. As a result, questionable extrapolations to process conditions must be performed.

Below, we describe a new electrokinetic technique that utilizes ultrasonics and preliminary data on the application of this technique to coal dispersions. The advantage of ultrasonics are (i) virtually any particle size can be used from ions to aggregates, (ii) any concentration of the dispersed phase can be used from the ppm range to volume filling networks, (iii) samples can be optically opaque or photosensitive, and (iv) measurements can be made on flowing systems.

William B. Russel

Department of Chemical Engineering
Princeton University
Princeton, NJ 08544

Recent Publications:

"The rheology of latices phase separated by dextran", J. Rheology 31, 599 (1987) [with P. D. Patel].

"Effective medium approximation for an elastic network model of flocculated suspensions", J. Rheology 31, 651 (1987) [with S. Mall].

"The rheological consequences of hydrodynamic interactions in dilute suspensions of rigid rods", J. Fluid Mech. 180, 475 (1987) [with D. H. Berry].

In Press:

"The dichroism and birefringence of a hard-sphere suspension under shear", J. Chem. Phys. [with N. J. Wagner and G. C. Fuller]

ABSTRACT

Optical measurements were used to detect structural anisotropy in concentrated dispersions over a range of Peclet numbers. Silica spheres of 49 and 130 nm radii with grafted octadecyl chains were dispersed in cyclohexane at volume fractions from 0.1 to 0.4. The apparatus consisted of a Couette cell with the dispersion in the annulus probed by a HeNe laser beam parallel to the axis of rotation. The dichroism and birefringence of the transmitted beam varied linearly with shear rate at low Peclet numbers with an orientation coincident with the principle direction of shear. Increasing the Peclet number, by increasing the particle size, produced a nonlinear response with the orientation tending to align in the direction of flow. A theory coupling the nonequilibrium microstructure under shear to the optical properties of the suspension enables direct interpretation of the dichroism. Comparison of sample dichroism calculations for two different forms of the theory demonstrates that the optical technique can be used to discriminate between theories which predict the microstructure.

"Self-consistent field model of polymer adsorption: Matched asymptotic expansion describing tails", Macromolecules [with H. J. Ploehn]

Abstract

General self-consistent field equations, derived previously, are solved within a perturbation scheme for the configuration probability of polymer chains. Building upon an earlier groundstate solution which describes adsorption in an "inner" region but precludes the prediction of tails, an "outer" region solution is developed herein as the lowest order-term in a perturbation expansion of the configuration probability in powers of reciprocal chain length. This solution is asymptotically matched with the inner (groundstate) solution, yielding a uniformly valid approximation. From this solution, we derive an analytical expression for the polymer volume fraction profile, including contributions due to segments contained in loops, tails, and non-adsorbed chains. Predictions for the adsorbed amount of polymer and hydrodynamic layer thickness agree quantitatively with experimental data, but agreement for the ellipsometric layer thickness is only qualitative. We describe the variation of chain configuration statistics (e.g. the distribution of segments in trains, loops, and tails) with experimental parameters. These results are analyzed using simple thermodynamic arguments.

FROM: Vivian T. Stannett
Department of Chemical Engineering
North Carolina State University
Raleigh, North Carolina 27695-7905

Promises, promises, promises! I can finally say that we have some data concerning our reverse emulsion polymerization of N-vinyl pyrrolidone. Unfortunately, we have only the one Ph.D. student (Maylon B. Taylor) and he is now part-time. We do however have three professors! --Myself, Richard D. Gilbert and Joel L. Williams.

We have conducted the polymerization at rather low ~12% monomer concentration in an isoparaffin oil. The monomer is about 50/50 in water and the initiation with gamma radiation. The latter appears to be very effective with inverse emulsion systems. The choice of emulsifier with such systems is critical and non-ionics such as the sorbital esters work well. Almost no polymerization takes place in the hydrocarbon phase. The system we use is very sensitive to traces of oxygen and for detailed kinetic studies argon or vacuum work the best. An end over end system somewhat similar to one described previously was used (K. Ishigure, T. O'Neil, E. P. Stahel and V. T. Stannett, J. Macromol. Sci-Chem A8 353 (1974) and gave good results.

Excellent yields at low total doses were obtained, for example 90% conversion at less than 2 Mrads. The practical objective was to obtain very high molecular weight polyvinyl pyrrolidone and this was achieved the highest being about 3×10^6 viscosity average. Since radiation is used as the initiating system, gelation is always a problem and care must be taken if high conversions are to be reached with the polymer to still be water soluble.

The work is still very much in progress and it is hoped that we will be able to give a more detailed report in six months.

dnus0425.1s8

Contribution to the Polymer Colloids Group Newsletter
Spring 1988

Polymer Research Laboratory
University of New Hampshire

Donald C. Sundberg

Morphology Control in Polymeric Microparticles

Since our last report we have studied the particle morphology resulting from combinations of a number of polymers, hydrocarbon oils and surfactants in aqueous dispersions. The experimental technique has been to dissolve the insoluble polymer/polymer or polymer/oil pairs in a mutual solvent, emulsify in water containing a surfactant, and to view the particle morphology development in the microscope as the solvent evaporates. As such, both still photography and video taping can be done to record the time dependent morphology. We have chosen to work with amorphous polymers and oils of greatly varying polarities, and surfactants with dramatically different surface activities (i.e. depression of interfacial tension). Some interesting results have been obtained for the materials shown below.

<u>Component</u>	<u>Fractional Polarity*</u>
PSty	0.17
PSAN (23% AN)	0.20
PSAN (33% AN)	0.22
PMMA	0.28
n-decane	0.00
1-decanol	0.26

*fractional polarity of water is about 0.7

Sodium lauryl sulfate (SLS) and a natural pectin (Mexpectin XSS100, or MXP) have dramatically different effects upon the water/organic interfacial tensions for the above materials and can thus play a large role in determining the morphology of the particle. Some interesting results are shown in the table below.

Component 1 → Surfactant	n-decane		1-decanol	
	MXP	SLS	MXP	SLS
Component 2 ↓				
PSty	1	2	2	2
PSAN (23%)	1	3	2	2
PSAN (33%)	1	3	2	2
PMMA	1	3	2	2

where 1 indicates core-shell particle, polymer as shell
 2 indicates core-shell particle, oil as shell
 3 indicates hemispherical particle

From these results we have learned that the final morphology is controlled by the particular combinations of interfacial tensions that exist for each system. Combinations of n-decane with the polymers result in markedly different morphologies when SLS is replaced by MXP as surfactant. When 1-decanol is used in combination with the polymers, the choice of surfactant has no effect due to the dominance of the 1-decanol/water interfacial tension.

The morphologies described above can be predicted using the concept of the minimization of interfacial free energy, as long as the various interfacial tensions can be reasonably approximated. Such predictions are in agreement with experiment when the morphology is allowed to develop slowly, i.e. the solvent is removed slowly. When the solvent is removed very rapidly, one can achieve morphologies which are very different from the ones shown in the above table. For example, one can achieve a core-shell morphology for the PMMA/n-decane/SLS system if the solvent is removed rapidly, but will obtain the hemisphere shape when the solvent is removed slowly. Thus we have begun to use the terms "equilibrium morphology" and "rate limited morphology" to describe our results.

Contribution to the Polymer Colloid Newsletter submitted by A.Vrij

- a) **HARD SPHERE DISPERSIONS: SMALL-WAVE-VECTOR STRUCTURE-FACTOR MEASUREMENTS IN A LINEAR SHEAR FLOW.**

Bruce J. Ackerson*, Jos van der Werff and C.G. de Kruif,

Van 't Hoff Laboratorium, Rijksuniversiteit Utrecht, 3508 TB Utrecht, the Netherlands.

*Permanent address: Department of Physics, Oklahoma State University, Stillwater, Oklahoma 74078, U.S.A.

Small scattering wavevector structure factor measurements have been made for model hard sphere suspensions undergoing a steady linear shear flow. The samples are comprised of sterically stabilized silica particles in cyclohexane and have been well characterized previously by rheological, by light scattering and by neutron scattering measurements. These combined measurements provide a strict test of recent theories of microscopic order in suspensions undergoing shear and suggest a picture which unifies several intuitive notions about suspensions undergoing shear flow: distortion of the pair correlation function, clustering, layering and nonequilibrium phase transitions.

Accepted: Phys. Rev. A.

- b. **ADHESIVE HARD-SPHERE COLLOIDAL DISPERSIONS, A SMALL-ANGLE NEUTRON SCATTERING STUDY OF STICKINESS AND THE STRUCTURE FACTOR.**

C.G. de Kruif¹, P.W. Rouw¹, W.J. Briels², M.H.G. Duits¹, A. Vrij¹, R.P. May³.

¹) Van 't Hoff Laboratory, University of Utrecht, Padualaan 8, De Uithof, 3584 CH Utrecht, The Netherlands.

²) University of Twente, Chemical Physics Lab., P.O. Box 217, 7500 AE Enschede

³) Institut Laue Langevin, BP 156X, F-3804, Grenoble Cedex.

Abstract:

Small angle neutron scattering structure factor measurements were made on sterically stabilized silica spheres dispersed in benzene up to volume fractions of 0.30. Benzene is only a marginal solvent for the stabilizing layer on the surface of the particles. The particles are made attractive by lowering temperature. This attraction is modelled by a square well potential the depth of which varies with temperature. At the highest temperature studied, our experimental system behaved effectively as an assembly of hard spheres, whereas at the lowest temperature the system approaches a spinodal. Using Baxter's theory we were able to evaluate the interaction parameters and to calculate the structure factor. Experiments were satisfactorily reproduced over the entire temperature range studied.

c. HARD-SPHERE COLLOIDAL DISPERSIONS: THE SCALING OF RHEOLOGICAL PROPERTIES WITH PARTICLE SIZE, VOLUME FRACTION AND SHEAR RATE.

J.C. van der Werff and C.G. de Kruif, Van 't Hoff Laboratorium, Transitorium III, Padualaan 8, 3584 CH Utrecht, The Netherlands.

Synopsis:

The steady-shear rheological properties of four sub-micron sterically stabilized silica dispersions differing in particle size were measured. The high and low shear limiting viscosities were found to be a function of the volume fraction only and the volume fraction at which the viscosity diverges was found to be $\phi_m = 0.63 \pm 0.02$ in the low shear limit and $\phi_m = 0.71 \pm 0.02$ in the high shear limit, independent of particle size. The shear thinning behaviour scales in the Peclet number. At higher volume fractions, the shear thinning transition shifts to a lower Peclet number. The time-scale on which the shear thinning transition takes place is comparable to the time-scale of short-time self diffusion i.e. D_s^{short} / a^2 and relates to the structural changes in the dispersion which were observed in an earlier rhe-optical study.

Submitted to: J. of Rheology

Activities in Trondheim

SINTEF, Institute of Industrial Chemistry.

Most of our activities are for the moment connected with biochemical and biomedical application of monodisperse polymer particles, especially magnetizable ones, and the modification of the particles to give the desired surface properties.

Below is summarized some important fields of application.

1. The papers concerning with magnetic particles mostly deal with the M-450 particle a 4,5 μm particle, which is you may say our basic particle.

The most exciting new areas of application of magnetic particles are:

1.1 Particles for isolation and studies of subcellular compartments.

A monosized particle with a shell has been developed which gives zero nonspecific binding.

1.2 Particles for DNA probe.

We have developed a particle which is especially suited for highly specific binding of single stranded DNA molecules.

1.3. Particles suitable for positive cell separation.

At several meetings, last time at the Gordon Conference, I have discussed the problem of positive cell separation, that is the problem of loosening the particles from the cells after isolation. We have lately, mainly through the work of dr.med. Kjell Nustad, come a long way on a road which we have reason to believe may solve the problem. Dr. Nustad may be able to present this work which involves some special pretreatment of the particles at the meeting in Strassbourg. Dr. Nustad will replace me to give the paper on biomedical application of monodisperse particles at the meeting.

2. Particles for studies of many body interactions.

We have continued our cooperation with Dr. Skjeltrorp at the Institute of Energy Technology, Kjeller, Norway on the use of monodisperse particles as models for studies of physical phenomena.

Dr. Skjeltrorp steadily finds new applications of monosized particles and is able to demonstrate and study sophisticated physical processes in an elegant and at the same time experimentally simple way. A light microscope is the main instrument applied.

The most recent work in this matter deals with dimensional modelling of:

- Porous materials (random to crystalline packing)
- Growth of aggregates, dendrites and faceted crystals
- Physical processes in porous materials like crystal growth, fracturing, diffusion and granular and fluid flow.

The types of monodisperse particles used for the above studies include compact and porous particles both magnetic and non magnetic. Spherical as well as non spherical particles are applied.

Dr. Skjeltorps' work will be presented in Strassbourg by Dr. Arvid Berge.

It has now been published more than 200 papers on the application of our monosized magnetic particles mainly in the medical field and an the use of monosized particles in studies of physical phenomena.

FREEZE FRACTURE ELECTRON MICROSCOPY
STUDIES OF POLYMER COLLOID MORPHOLOGY

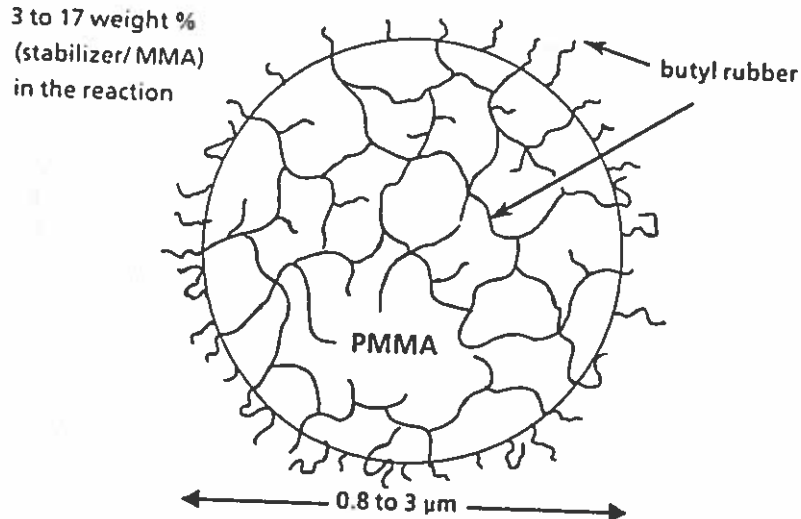
M.A. Winnik,^{*} B. Disanayaka,^{*} R.R. Shivers[†] and M.D. Croucher^{**}

(^{*}) Department of Chemistry, University of Toronto, Toronto, Ontario, Canada, M5S 1A1; ([†]) Department of Zoology, University of Western Ontario, London, Ontario, Canada, N6A 3K7; (^{**}) Xerox Research Centre of Canada, 2660 Speakman Drive, Mississauga, Ontario, Canada, L5K 2L1.

We wish to report some important preliminary results on particle morphology which have been obtained by applying the freeze-fracture electron-microscopy technique to the study of NAD particles. Over the past several years we have been studying an NAD system obtained by polymerizing methyl methacrylate [MMA] in isooctane in the presence of butyl rubber [polyisobutylene-co-polyisoprene (1%), PIB]. These reactions yield sterically stabilized dispersions of narrow size distribution. Through manipulation of the reaction conditions, particles with diameters of 0.7 to 3 μm are obtained. The composition of these particles varies with the reaction conditions, and they are found to contain from 1 to 10 monomer mol% PIB, present as a graft copolymer with PMMA. From sorption experiments, where sorption was followed by a fluorescence quenching technique, we inferred that these particles have an interpenetrating network structure. Our view of this structure is given in Figure 1. We have had occasion recently to publish several reviews of this work.¹⁻⁴

Very recently we have had the opportunity to study these materials using the technique of freeze-fracture electron microscopy,⁵ with the experiments carried out in the laboratory of R.R. Shivers at the University of Western Ontario. Here we report results on particles suspended in glycerol in the presence of Triton X-100. Particles were frozen to 77°K in contact with Freon to insure rapid heat transfer and then immersed in liquid nitrogen. After

Figure 1



cleavage, a mask of platinum (400 Å to 600 Å thick) was prepared by vapor deposition onto the cold substrate using classical shadowing techniques. After thawing, the polymer sample was removed from the mask using chloroform. The cleaned Pt masks were examined by high resolution electron microscopy. The ultimate resolution obtainable is determined by the size of the metal cluster which deposits from the vapor phase. For Pt, this limit is ca. 20 Å.

As a control we examined a PMMA emulsion particle, 500 nm in diameter, obtained from Seragen Diagnostics (now Seradyn, Inc). A typical example is shown in Figure 2. These particles tend to break like cupcakes, exposing convex and concave internal surfaces. The fine structure seen in the EM photographs may not be evident in the photocopies of this report which are circulated as part of the Newsletter. What one sees is that the internal structure resembles that of a "bag of marbles": The fracture surface seems to be made up of grains resembling tiny spheres ca. 80 Å in diameter, densely packed but without any obvious indication of regular close packing.

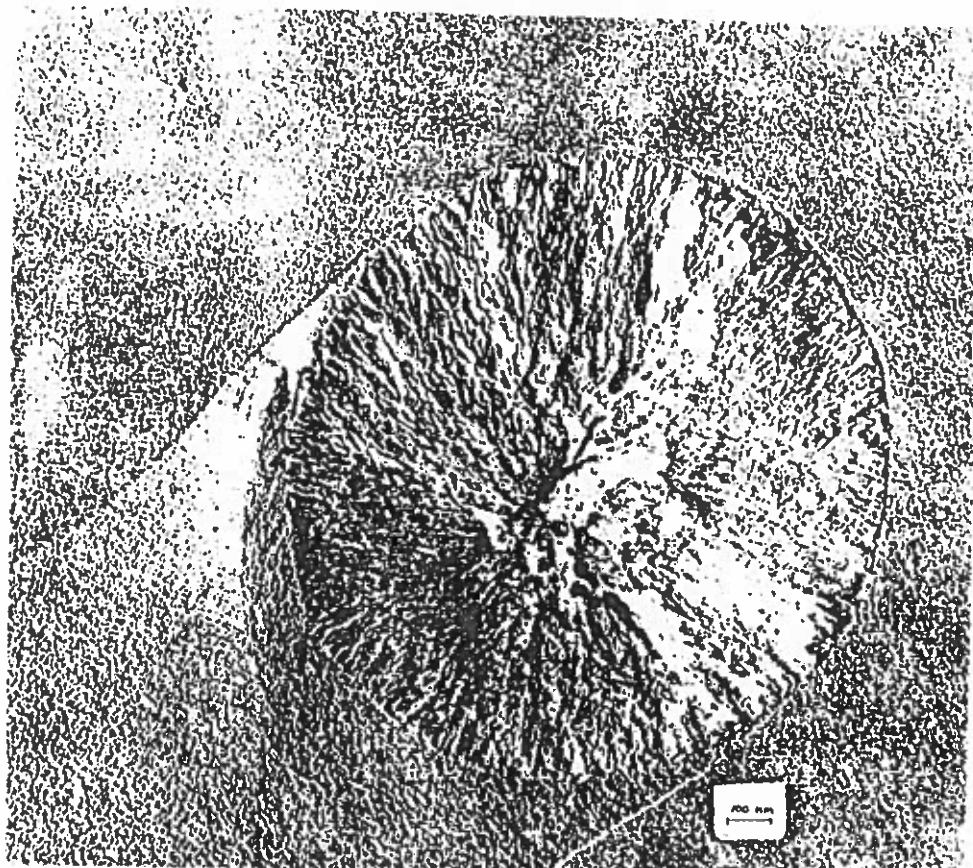


Figure 2

The NAD particles have a completely different morphology, Figure 3. Two features of the micrograph are striking. First, almost all particles cleave through their centres. Second, the fracture surface is rugged and richly textured. It has the texture of mountain ranges, viewed from above, emanating from a central feature. These emanations are globally radiant, but appear in such a variety of patterns that no two particles interiors appear identical. One is reminded of snowflakes, which have global characteristics in common, but a seemingly infinite variety of local patterns.

We interpret these freeze fracture electron micrographs to indicate the disposition of the PIB phase trapped in the core of the particle. It is well known in freeze-fracture microscopy that cleavage occurs along surfaces of least resistance. In our view these surfaces are the PIB-PMMA interfaces. The implication of these results is that although the amount of PIB contained

Figure 3



in the particles is small (here 1.5 mol%), it is distributed over an enormous surface area. This surface area would be a maximum if the PIB were present locally in the form of a monolayer.

While few doubt that the surface of sterically stabilized particles contain a monolayer of stabilizer, the idea that the stabilizer polymer trapped inside the particle is also distributed in monolayer form seems a bit strange. This extreme view, nevertheless, is supported by the other kinds of experiments. There are new ways of carrying out energy transfer experiments which allow one to assess the local dimensionality of the phase in which the fluorescent dyes are dispersed. When appropriate dyes are dissolved in the PIB phase of this material, these direct energy transfer experiments show that on a scale of ca. 40 Å, the PIB phase is locally two dimensional.

Morphology provides powerful insights into the mechanism of particle

formation. Our view of this process is the following: Polymerization of MMA in solution is competitive with hydrogen abstraction from PIB leading to graft copolymer formation. In the early stages of the reaction when little graft copolymer is present, primary PMMA particles are not stabilized against aggregation. As the reaction proceeds, graft copolymer adheres to the surface of both primary particles and aggregates. These are swollen with monomer, and after 10% conversion, much of the subsequent polymerization of MMA occurs inside the swollen polymer phase. Particle growth exposes new surface area and promotes aggregation of units containing a monolayer coverage of the PIB-PMMA graft copolymer. As a consequence, some of the PIB component becomes trapped within the aggregates and forms the PIB network in the final particle.

Other features of the morphology appear in the electron micrographs when the particles are dispersed in hydrocarbon fluids and then frozen. The hydrocarbons swell the PIB phase of the particles as well as the graft-copolymer interphase adjacent to the PIB layer. While there is a lot of information contained in these micrographs, we do not yet understand all that we see. As we come to understand these results, we will submit them for publication.

REFERENCES

1. M.A. Winnik and M.D. Croucher, "The Characterization of Polymer Colloids by Fluorescence Quenching Techniques," in "Future Directions in Polymer Colloids," M.S. El-Aasser, Ed., Martinus Nijhoff Publishers, Dordrecht, The Netherlands, 1987.
2. M.D. Croucher and M.A. Winnik, "Control of Particle Size in the Dispersion Polymerization of Sterically Stabilized Polymer Colloids," in "Future Directions in Polymer Colloids," M.S. El-Aasser, Ed., Martinus Nijhoff Publishers, Dordrecht, The Netherlands, 1987.
3. M.A. Winnik, "The Study of Complex Polymer Materials by Fluorescence Quenching Techniques," in "Photophysics of Polymers," C.A. Hoyle, editor, ACS Symposium Series 358, Chapt. 2, 1987.
4. M.A. Winnik, in 'Photophysical and Photochemical Tools in Polymer Science', M.A. Winnik, editor, D. Reidel Publishers, Dordrecht, Holland, 1986.
5. (a) W.F. Dunlop and A.W. Robards, J. Ultrastructure Research, 40, 391 (1972); (b) see also R.F. Stewart and D. Sutton, Chem. and Ind., 21 May 1984, p.373.
6. Ö. Pekcan, M.A. Winnik, and M.D. Croucher, to be published.